SURE 静岡大学学術リポジトリ
Shizuoka University REpository

Floral organ- and temperature-dependent regulation of anthocyanin biosynthesis in Cymbidium hybrid flowers

メタデータ	言語: eng 出版者: 公開日: 2019-07-24 キーワード (Ja): キーワード (En): 作成者: Nakatsuka, Takashi, Suzuki, Tomohiro, Harada, Kenji, Kobayashi, Yuki, Dohra, Hideo, Ohno, Hajime メールアドレス: 所属:
URL	http://hdl.handle.net/10297/00026724

Floral organ- and temperature-dependent regulation of anthocyanin biosynthesis in *Cymbidium* hybrid flowers

Takashi Nakatsuka [1,2,*], Tomohiro Suzuki [3,4], Kenji Harada [1], Yuki Kobayashi [1], Hideo Dohra [3], Hajime Ohno [1,2]

[1] Faculty of Agriculture, Shizuoka University, Shizuoka 422-8529 Japan

[2] College of Agriculture, Academic Institute, Shizuoka University, Shizuoka 422-8529 Japan

[3] Research Institute of Green Science and Technology, Shizuoka University, Shizuoka 422-8529 Japan

[4] Center for Bioscience Research and Education, Utsunomiya University, Utsunomiya 321-8508 Japan

[*] **Corresponding author**

Takashi Nakatsuka, Ph. D.

College of Agriculture, Academic Institute, Shizuoka University, 836 Ohya Suruga-ku Shizuoka, 422-8529 Japan

Tel & Fax: +81-54-238-4353

e-mail**:** nakatsuka.takashi@shizuoka.ac.jp

Abstract

Anthocyanins are responsible for red, purple, and pink pigmentation of flowers in *Cymbidium* hybrids. Although anthocyanin content in all floral organs increases with flower development, they increase markedly in the tepals compared with the labella or

columns. Using next-generation sequencing technology, we identified three anthocyanin biosynthesis regulatory genes, *CyMYB1*, *CybHLH1*, and *CybHLH2*, from *Cymbidium* 'Mystique'. Yeast two-hybrid analysis showed that the CyMYB1 protein can form a heterodimer with either CybHLH1 or CybHLH2. In the tepals, the expression level of *CyMYB1* increased as the flower developed, whereas the high expression level of *CyMYB1* was detected at the early flower developmental stages in the labella and columns, remaining constant until increasing at the late developmental stage. These expression profiles of *CyMYB1* positively correlated with the profiles of anthocyanin accumulation in the tepals. When *Cymbidium* Sazanami 'Champion' was grown at 30°C/25°C, reduced anthocyanin levels were observed, specifically in the tepals, compared with those in flowers grown at 20°C/15°C. The transcription of *CyMYB1* in the tepals was suppressed at high temperatures, and the expressions of *CyDFR* and *CyANS* were also synchronously suppressed. This study revealed that *CyMYB1* activates the transcription of *CyDFR* and *CyANS* and regulates the temporal- and temperature-dependent anthocyanin accumulation in *Cymbidium* tepals.

Keywords

Anthocyanin**,** high temperature**,** RNA-Seq**,** R2R3-MYB

Abbreviations

3GT anthocyanidin 3-*O*-glucosyltransferase,

3RT anthocyanidin 3-*O*-glucoside rhamnosyltransferase

ANS anthocyanidin synthase

bHLH basic Helix-Loop-Helix

CHS chalcone synthase

CHI chalcone isomerase

Cy3G cyanidin 3-*O*-glucoside

Cy3R cyanidin 3-*O*-malonylglucoside

Cy3R cyanidin 3-*O*-rutinoside

DFR dihydroflavonol 4-reductase

EFP enhancer of flavonoid production

F3H flavanone 3-hydroxylase

F3′H flavonoid 3′-hydroxylase

FLS flavonol synthase

HPLC high performance liquid chromatography

MalT anthocyanin:malonyl-CoA acyltransferase

Pe3R peonidin 3-*O*- rutinoside

qPCR quantitative polymerase chain reaction

WDR WD40 repeat

1. Introduction

Cymbidium spp. is one of the most commercially popular orchids, along with *Phalaenopsis* spp., and is utilized as a cut flower or potted plant in floriculture worldwide. The genus *Cymbidium* is a member of the Orchidaceae family containing approximately 700 genera, and consists of 44 species, which are distributed across tropical and subtropical Asia and northern Australia (Arditti, 1992). *Cymbidium* has been grown as a cultivated plant for over one hundred years, and remains, to the present day, one of the most important orchids in commerce.

Cymbidium flowers are composed of four different organs of different forms, including three petal-like sepals, two lateral petals, one labellum, and one column organ. The morphogenetic characters of the petal-like sepals are so similar to those of the lateral

petals that both are called tepals, whereas the structure of the labellum organ is significantly different from that of the other flower organs (Figs. 1A and B).

Cymbidium hybrid cultivars exhibit a range of flower colors, including white, pink, red, purple, yellow, and green [1]. Of these, anthocyanin accumulation is responsible for pink, red, and purple flower colorations, whereas carotenoid and chlorophyll accumulations are responsible for yellow and green colorations, respectively, in the floral organs of *Cymbidium* [2]. Cyanidin 3-*O*-glucoside, cyanidin 3-*O*-rutinoside, and cyanidin 3-*O*-(6″-malonylglucoside) have been identified as the major anthocyanins in cyanic *Cymbidium* cultivars [1].

Anthocyanin biosynthesis has been well studied in model plants, including *Arabidopsis thaliana*, *Zea mays*, *Antirrhinum majus*, and *Petunia hybrida* [3, 4]. Several studies have been reported the molecular biology of flower pigmentation in other genera of the Orchidaceae family, namely *Oncidium* [5-7] and *Phalaenopsis* [8]. However, there have been few reports of differential expression analysis of anthocyanin biosynthetic genes in *Cymbidium* hybrids. The dihydroflavonol 4-reductase (DFR)-encoding gene was isolated from a *Cymbidium* hybrid and shown to be unable to reduce dihydromyricetin to leucodelphinidin [9]. The genes encoding chalcone synthase (CHS), flavonol synthase (FLS), flavonoid 3′-hydroxylase (F3′H), and anthocyanidin synthase (ANS) have also been identified from a *Cymbidium* hybrid [10]. However, in the putative anthocyanin biosynthetic pathway in *Cymbidium* floral organs illustrated in Supplementary Fig. S1, the genes encoding chalcone isomerase (CHI), flavanone 3-hydroxylase (F3H), anthocyanidin 3-*O*-glucosyltransferase (3GT), anthocyanidin 3-*O*-glucoside rhamnosyltransferase (3RT), and anthocyanin: malonyl-CoA acyltransferase (MalT) have still to be isolated and identified.

It is known that the regulation of anthocyanin biosynthesis is controlled by the MYB-

bHLH-WDR complex composed of three proteins, namely the R2R3-MYB, the basic Helix-Loop-Helix (bHLH), and the WD40 repeat (WDR) proteins [11, 12]. In the Orchidaceae family, it has also been reported that the floral pigmentation of *Oncidium* is regulated by *OsMYB1* [5, 6]. The flower coloration and color patterning of *Phalaenopsis* are also regulated by three R2R3-MYB genes, namely *PeMYB2*, *PeMYB11*, and *PeMYB12* [8]. In a *Dendrobium* hybrid, *DhMYB2* and *DhbHLH1* are responsible for regulating anthocyanin biosynthesis [13]. When the *Leaf color* (*Lc*, bHLH) and *Colorless 1* (*C1*, MYB) genes from *Z. mays* were transiently expressed in white-flowered petals of the *Cymbidium* hybrid 'Jung Frau dos Pueblos', anthocyanin-producing cells were observed [14]. Therefore, the regulation of anthocyanin accumulation in *Cymbidium* petals could be controlled by the MYB/bHLH complex. However, although the regulatory genes of anthocyanin biosynthesis have been identified in other Orchidaceae members, no research has yet been reported in *Cymbidium.* Transcriptome sequence data of 11 orchid species are available at OrchidBase [15, 16]. The genome sequence of *Phalaenopsis equestris* has also been published [17], while the molecular biology characteristics of *Cymbidium ensifolium* have also been studied in terms of transcriptome [18-20] and proteome [21]. *C. ensifolium* is one of the parent species involved in the breeding of *Cymbidium* hybrids, but anthocyanin accumulation was not observed in its tepal organs. Therefore, there is no molecular genetic resource available for analysis of the genes regulating flower pigmentation in *Cymbidium* hybrid cultivars. Expressed-sequence tag sequencing using next-generation sequencing has been utilized to identify several genes related to important floral traits of horticultural plants where genome information is lacking [22-24].

It has long been known that growth temperature conditions affect anthocyanin accumulation levels in the petals of petunia [25, 26], chrysanthemum [27], aster [28], rose

[29], and lily [30], in the fruits of apple [31] and grape [32], and in the seedlings of *Arabidopsis* [33] and maize [34]. Generally, moderate to low temperatures increase anthocyanin accumulation, whereas high temperatures decrease it [35]. *Cymbidium* plants usually bloom during the winter in Japan. Therefore, the flower color intensity of *Cymbidium* may also be affected by the growth temperature, but this has not yet been studied.

Here, we identified the anthocyanin biosynthetic regulatory gene *CyMYB1* from a *Cymbidium* hybrid using next-generation sequencing and revealed that the expression of *CyMYB1* was suppressed at high temperatures, leading to reduced anthocyanin accumulation in the tepals of *Cymbidium*.

2. Materials and Methods

2.1. Plant materials

Plants of the *Cymbidium* hybrid 'Mystique' were grown in a field of Shizuoka University, Japan. Three floral organs, namely the tepal, the labellum, and the column (Fig. 1A), were collected, snap-frozen immediately in liquid nitrogen, and stored separately at −80°C until they were used. Flowers were collected at four floral development stages as follows: stage 1 (S1), perianth height, 15 to 20 mm; S2, perianth height, 20 to 25 mm; S3, perianth height, 25 to 30 mm; and S4, anthesis (Fig. 1B).

Cymbidium Sazanami 'Champion' was also used to investigate the effects of the growing temperature on flavonoid accumulation and expression of the corresponding biosynthetic genes. The flower pigmentation of this cultivar responded more to the growth temperature than did 'Mystique'. *Cymbidium* Sazanami 'Champion' plants with S2-flower buds growing in pots were transferred to two different growth chambers, namely at low- (20°C/15°C day/night) and high-temperature conditions (30°C/25°C), under a 12-

h photoperiod, with light supplied by a high-pressure sodium lamp.

2.2 Flavonoid analysis

A sample (100 mg fresh weight) of each organ was powdered using liquid nitrogen and then extracted in 1 mL of extraction solution containing 40% (v/v) methanol and 10% (v/v) acetic acid, for 24 h at 4°C. The extract was then filtered by passage through a 0.22-μm PTFE syringe filter (Osaka Chemical, Osaka, Japan). Anthocyanin and flavonol analyses were carried out by the Agilent Infinity 1290 HPLC system (Agilent Technologies, Santa Clara, CA, USA) with an Agilent 1200 Diode-Array Detector SL (Agilent Technologies), and a reversed-phase column ZORBAX SB-C18 (2.1 × 50 mm, 1.8 μm). Two solvents, solvent A (1.5% [v/v] phosphoric acid) and solvent B (1.5% [v/v] phosphoric acid containing 20% (v/v) acetic acid and 25% (v/v) acetonitrile), were used for elution at 40°C at a flow rate of 1.0 mL min^{-1}. The elution was performed with 10% solvent A for 1 min, and then increasing to 60% solvent A for 8 min using gradient. Anthocyanins and flavonols were monitored as absorbance at 525 and 360 nm, respectively. The anthocyanin concentration was calculated using standards (cyanidin 3-*O*-glucoside and cyanidin 3-*O*-rhamnoside; Extrasynthese, Lyon, France). Since a standard of cyanidin 3-*O*-malonyglucoside was not commercially available, the concentration of this molecule was calculated using a standard curve of cyanidin-3-*O*-glucoside. The flavonol concentration was calculated from area of all peaks detected at 360 nm.

2.3. Construction of a cDNA library from **Cymbidium** *labella*

Total RNAs were isolated from labella of *Cymbidium* ‘Mystique’ using RNAiso Plus (Takara Bio, Shiga, Japan) with Fruit-mate for RNA Purification (Takara Bio), and then

176 treated with DNase I to remove any remaining genomic DNA. The cDNA library was
177 synthesized using the SureSelect Strand-Specific RNA Library Prep for Illumina
178 Multiplexed Sequencing (Agilent Technologies) according to the manufacturer's
179 instructions. The library obtained was adjusted to a concentration of 20 pM, and
180 sequencing was performed with 2 × 75-bp paired-end reads on the Illumina MiSeq Next-
181 Generation Sequencer (Illumina). The adapters and other low-quality reads were removed
182 from the raw sequence data using cutadapt (version 1.8.1) [36] to trim low-quality ends
183 (<QV30), the 76th nucleotides, and adapter sequences, and to discard reads shorter than
184 50 bp, and the clean reads were assembled using Trinity software version r20140413p1
185 [37]. The contigs obtained were defined as unigenes after removing any redundancy.
186 These unigenes were submitted to the *Arabidopsis* protein database TAIR10 (The
187 Arabidopsis Information Resource [TAIR]) for homology and annotation comparison by
188 the BLASTX algorithm and by InterPro. The Blast2GO program [38] was used in GO
189 annotation and functional classification.
190
191 ***2.4. Isolation of anthocyanin biosynthesis genes from* Cymbidium**
192 The putative open reading frames (ORFs) of the *Cymbidium* anthocyanin
193 biosynthesis genes were expected to be obtained from the *Cymbidium* cDNA library.
194 However, many contigs did not contain the complete coding region. Therefore, we used
195 the rapid amplification of cDNA ends technology to obtain full-length cDNA sequences
196 using the GeneRacer Kit (Invitrogen, by Thermo Fisher Scientific, Carlsbad, CA, USA).
197 The ORF sequences were amplified using Takara *Ex-Taq* polymerase (Takara Bio), and
198 the primer sets are shown in Supplementary Table S1. The thermal cycler program was
199 set as follows: 94°C for 2 min, then 35 cycles of 94°C for 20 s, 60°C for 40 s, and 72°C
200 for 2 min, and a last step at 72°C for 10 min. The amplified fragments were purified using

Wizard SV gel and PCR Clean-Up System (Promega, Madison, WI, USA), and were subcloned into the pGEM-Teasy vector system (Promega). The sequences of all constructs were confirmed by DNA sequencing (Fasmac, Kanagawa, Japan). For phylogenetic analysis of the CyMYBs, the deduced amino acid sequences of the R2R3 domain of CyMYBs were aligned with R2R3-MYBs from other species using ClustalW [39]. A phylogenetic tree was constructed by Molecular Evolutionary Genetics Analysis version 6.0 (MEGA6) using the neighbor-joining method with 1,000 bootstrapping data sets [40].

2.5. Gene expression analysis

Total RNAs were isolated from each floral organ of *Cymbidium* 'Mystique' at the different developmental stages described above. The elimination of genomic DNA and cDNA synthesis were carried out using the PrimeScript RT Reagent Kit with gDNA Eraser (Takara Bio). Quantitative real time PCR (qPCR) analysis of each gene was performed with Thermal Cycler Dice Real Time System (TP850; Takara Bio) using the KAPA SYBR FAST qPCR Master Mix kit (KAPA Biosystems, Wilmington, MA, USA). Briefly, the reaction mixture (10 μL) consisted of 1× Master Mix, 0.2 μM each primer, and 1 μL template cDNA. The cycling conditions were as follows: 95°C for 20 s, followed by 40 cycles of 95°C for 1 s and 60°C for 20 s. The specificity of each amplification reaction was checked by the addition of a dissociation analysis step after the cycle reaction. The data were analyzed by second derivative maximum methods using the Thermal Cycler Dice Real Time System II software version 5.00 (Takara Bio). The transcript level of each gene was calculated relative to that of the *Cymbidium* actin-encoding *CyACT1* (LC424204) as a reference gene. The qPCR analyses were performed with six biological replicates. The sequences of all primers used in the qPCR analysis are

226 listed in supplementary Table S2.

227

228 ***2.6. Protein–protein interaction between CyMYB1 and CybHLHs***

229 To investigate the interactions among the CyMYB1, CybHLH1, and CybHLH2
230 proteins, we employed the yeast two-hybrid analysis using a Matchmaker Two-Hybrid
231 System 3 (Clontech, Takara Bio, Otsu, Shiga, Japan). The coding regions of *CyMYB1*,
232 *CybHLH1*, and *CybHLH2* were cloned into either the pGAD-T7 (GAL4 activation
233 domain) or pGBK-T7 (GAL4 DNA-binding domain) vector. All constructs were
234 transformed into *Saccharomyces cerevisiae* AH109 (Clontech, Takara Bio). The
235 transformed yeast cells were grown on SD selective medium without leucine (−Leu) and
236 tryptophan (−Trp) at 30°C for 3 days. The survival test for each transformed yeast culture
237 was performed on selective quadruple-dropout medium (−Leu, −Trp, histidine [−His],
238 and adenine [−Ade]) supplemented with 15 mM 3-amino-1,2,4-triazole (3-AT) at 30°C
239 for 3 days.

240

241 ***2.7. Statistical analysis***

242 Data are presented as mean ± SE. Statistical comparisons were carried out using the
243 Student's *t*-test.

244

245 **3. Results**

246 ***3.1. Isolation of anthocyanin biosynthesis-related genes using next-generation***
247 ***sequencing***

248 To construct a unigene catalog of *Cymbidium* 'Mystique' labella, we performed
249 RNA-Seq using 75-bp paired-end reads in Illumina MiSeq. After quality filtering and
250 read cleaning, we obtained approximately 16 million sequencing raw reads, from which

59,000 contigs were assembled with an average sequence length of 922 bp.

Based on either homology search by BLAST or domain search by InterPro, 15 contigs of the R2R3-MYB transcription factor were found in the *Cymbidium* ‘Mystique’ flower cDNA contigs. They were classified into each subfamily by phylogenetic analysis (Fig. 2). The deduced amino acid sequence of *CyMYB1* (DDBJ accession number LC422758) exhibited 70.6% and 71.2% identities with those of the *Oncidium* hybrid *MYB1* and *Arabidopsis thaliana TRANSPARENT TESTA 2* (*TT2*), respectively, which have been recognized to be anthocyanin biosynthesis regulators, and were categorized into the *C1* subfamily. In addition, CyMYB1 was categorized into a clade including anthocyanin biosynthesis-related R2R3-MYBs from other members of the Orchidaceae (Fig. 2). The bHLH interaction motif [D/E]Lx2[R/K]x3Lx6Lx3R [41] was well conserved within the R3 repeat domain of CyMYB1 (76^{th}–95^{th} residues).

Two *bHLH* orthologs, *CybHLH1* (LC422759) and *CybHLH2* (LC422760), were also found among the *Cymbidium* flower cDNA contigs (Supplementary Fig. S2). The deduced amino acid sequence of *CybHLH1* exhibited 76.9% identity with that of *CybHLH2*. Moreover, CybHLH1 and CybHLH2 exhibited 47.3% and 47.4% identities, respectively, with a *Dendrobium* hybrid DhbHLH1 (AQS79853, [13]). They also exhibited 49.1% and 49.0% identities with the *Lilium* hybrid bHLH (BAE20057, [42]). CybHLH1 and CybHLH2 were classified into a clade that included the *Lilium* hybrid bHLH1, which was different from the clade that contained the other orchid bHLHs (Supplementary Fig. S2). We attempted to identify an anthocyanin biosynthesis-related WDR *Arabidopsis* TTG1 but could identify no WDR ortholog from the *Cymbidium* flower cDNA contigs (data not shown).

In addition, we were successful in identifying anthocyanin biosynthesis genes, including *CyCHI* (LC422751), *CyCHI2*/*EFP* (LC422750), *CyF3H* (LC422752),

CyF3'H1 (LC422753), *CyF3'H2* (LC422754), *Cy3GT* (LC422755), *Cy3RT* (LC422756), and *CyMalT* (LC4227557) from *Cymbidium* (Supplementary Figs. S3–S7). Of these, the predicted amino acid sequences of the proteins encoded by two *F3'H* genes, *CyF3'H1* and *CyF3'H2*, exhibited low amino acid sequence similarity with the protein encoded by *ChF3'H* (KM186178), which had been previously reported by Wang et al. [10]. The deduced amino acid sequence of *CyF3'H1* exhibited 57.7% identity with that of *CyF3'H2*, and the sequences of *CyF3'H1* and *CyF3'H2* exhibited 51.9% and 54.7% identities, respectively, with the amino acid sequence of *ChF3'H* (Supplementary Fig. S5). These results suggest that sequence diversity seems to exist within the *F3'H* gene in *Cymbidium* hybrids.

3.2. Protein–protein interaction between CyMYB1 and CybHLHs

To investigate whether CyMYB1 interacts with either CybHLH1 or CybHLH2, we employed a GAL4-based yeast two-hybrid system (Fig. 3). All yeasts harboring GAL4 DNA-binding-domain-fused CyMYB1 grew in the quadruple-dropout medium, suggesting false positive results. The yeasts harboring the combination of CyMYB1 and either CybHLH1 or CybHLH2 survived on quadruple-dropout medium, and no difference in the growth speed was observed in either combination of CyMYB1 and either CybHLH1 or CybHLH2. The yeasts harboring the combination of CybHLH1 and CybHLH2 also showed low survival on quadruple-dropout medium, suggesting the formation of heterodimers or homodimers within/between CybHLH1 and CybHLH2. These results support the hypothesis that CyMYB1 and either CybHLH1 or CybHLH2 form a heterodimer, as reported for anthocyanin transcription factors from other plants [12].

3.3. Temporal changes of flavonoid accumulation and flavonoid biosynthetic gene expressions in Cymbidium *'Mystique' tepals*

The anthocyanin and flavonol concentrations in the tepals at different flower developmental stages were determined using HPLC. The major anthocyanins extracted from *Cymbidium* 'Mystique' flowers were three cyanidin derivatives, namely cyanidin 3-*O*-glucoside, cyanidin 3-*O*-rutinoside, and cyanidin 3-*O*-malonylglucoside, confirming the findings of Tatsuzawa et al. [1]. Total anthocyanin content per tepal increased to 21.8 μg during flower development and was closely associated with the development of tepal pigmentation (Figs. 1A and 1C). The three anthocyanin components, including cyanidin 3-*O*-glucoside, cyanidin 3-*O*-rutinoside, and cyanidin-3-*O*-malonylglucoside, were present in nearly equal ratios, and no change in the amounts occurred during floral development. The peak at retention time 3.45 min corresponded to the major flavonol compound and represented approximately 60% of the total flavonols in all organs during flower development (data not shown). However, because we could not identify the structure of this major compound, flavonol amount was shown by the peak area of chromatograms at 360 nm. In the tepals, the flavonol content at S4 increased to 1.9 times than that at S1 (Fig. 1D).

To investigate the expression profiles of putative flavonoid biosynthesis regulatory genes in the tepals during flower development in *Cymbidium* 'Mystique', we performed qPCR analysis (Fig. 4). The expression levels of *CyMYB1* increased in the tepals during floral development, with the maximum expression levels being achieved at the floral developmental stage 3 (S3). These temporal expression profiles closely correlated with those of anthocyanin accumulation in *Cymbidium* tepals (Fig. 1C). Conversely, *CybHLH1* and *CybHLH2* transcript abundance was constant from S1 flower developmental stage to stage 3 at which point they increased and decreased, respectively,

at stage 4 (Fig. 4). Therefore, neither *CybHLH1* nor *CybHLH2* exhibited the dynamic expression variation corresponding with the anthocyanin accumulation profiles in tepals as *CyMYB1* did.

In addition, we investigated the temporal expression profiles of the structural genes involved in anthocyanin and flavonol biosynthesis, including *CyCHS*, *CyCHI*, *CyEFP*, *CyF3H*, *CyFLS*, *CyF3'H1*, *CyF3'H2*, *CyDFR*, *CyANS*, *Cy3GT*, *Cy3RT*, and *CyMalT* in *Cymbidium* 'Mystique' tepals (Fig. 5). The temporal expression profiles of *CyCHS*, *CyF3H*, *CyF3'H2*, *CyDFR*, *CyANS* and *CyMalT* were relatively similar to the *CyMYB1* expression and anthocyanin accumulation profiles in the tepals (Figs. 1C, 4, and 5). These findings suggest that the expression of these anthocyanin biosynthesis genes is regulated by the *CyMYB1* transcription factor. Conversely, the high expression levels of *CyEFP* and *CyFLS* were detected in the tepals at all flower developmental stages (Fig. 5). The expression profiles of these two genes correlated well with that of *CybHLH2* and the flavonol accumulation profiles in the tepals (Figs. 1D and 5). The expression profiles of *3GT* and *3RT*, which encoded anthocyanin glycosyltransferases, did not correlate with either the anthocyanin or flavonol accumulation profile of any of the floral organs (Figs. 1D and 5).

3.4. Temporal changes of flavonoid accumulation and flavonoid biosynthetic gene expressions in Cymbidium *'Mystique' labella*

The total anthocyanin content per labellum was similar to that in the tepals at the flower developmental stage 1 and increased to 7.4 μg/organ at flower development stage 4 (Fig. 1C). Pigmentation was observed mainly at the upper parts of the labellum, with anthocyanin accumulating only slightly at the lower parts. The ratio of cyanidin 3-*O*-glucoside, cyanidin 3-*O*-rutinoside, and cyanidin-3-*O*-malonylglucoside was similar to

that in the tepals (Fig. 1C). Conversely, the flavonol content in the labellum at S1 was 52.3% compared with that in the tepal. However, the flavonol content of the labellum at S4 had increased to 3.7 times than that at S1, being similar to the flavonol content of the tepals at S4 (Fig. 1D).

Furthermore, we investigated the expression profiles of flavonoid biosynthesis-related genes in the labellum during flower development in *Cymbidium* 'Mystique' (Figs. 4 and 5). The abundance of *CyMYB1* transcripts was more-or-less constant from S1 to S3 in the labellum, before significantly decreasing at S4 (Fig. 4). Similarly, the expression levels of *CybHLH1* in the labellum did not change throughout flower development. Moreover, the expression of *CybHLH2* in the labellum was strongly detected at S1, and then decreased during later floral development. These temporal expression profiles did not closely correlate with those of anthocyanin accumulation in the *Cymbidium* labellum (Fig. 1C). The structural genes *CyDFR*, *CyANS*, and *CyMalT* were expressed at a constant level in the labellum from S1 to S3, and then, the expression significantly decreased at S4, indicating that the expression profiles of these three genes resembled that of *CyMYB1* (Figs. 4 and 5). In contrast, the expression of *CyCHI*, *CyEFP*, *CyF3H*, *CyF3'H2*, and *CyFLS* decreased as the flower developed, indicating that the expression profiles were similar to that of *CybHLH2* (Figs. 4 and 5). The expression levels of *CyEFP*, *CyF3H*, *CyF3'H2*, and *CyFLS* in the labellum at flower development S1 were significantly greater than those in the tepals and columns.

3.5. Temporal changes of flavonoid accumulation and flavonoid biosynthetic gene expressions in Cymbidium *'Mystique' columns*

Anthocyanin accumulation was under the detection level in the column at S1 (Fig. 1C). Anthocyanin accumulation started at the base of the column at S2, with total

anthocyanin content per column reaching a peak of 6.2 μg at S3. Peonidin 3-rutinoside, which was barely detectable in the tepals and labella, accumulated to 16.5% of the total anthocyanin content in the column (Fig. 1C). In addition, non-malonyl anthocyanins accounted for 79.2% of total column anthocyanins.

The temporal expression profiles of anthocyanin regulatory genes in the column were similar to those in the labellum than in the tepal (Fig. 4). The expression levels of *CyMYB1* and *CybHLH2* peaked at S2, and then decreased as the flower continued to develop. Conversely, *CybHLH1* was expressed constantly from S1 to S3, before increasing at S4 (Fig. 4). The regulatory gene expression profiles in the column did not correlate with either anthocyanin or flavonol accumulation profiles (Figs. 1C and 1D). The expressions of *CyDFR* and *CyANS* peaked at S2 in the labellum, before significantly decreasing at S4. The expression profiles of these two structural genes were similar to those of *CyMYB1* (Figs. 4 and 5). The maximum expression levels of *CyCHS*, *CyF3H*, and *CyF3'H2* in the column were significantly lower than those in either the tepals or labella.

3.6. Suppression of anthocyanin accumulation induced by high temperature

To investigate whether *CyMYB1* regulates anthocyanin biosynthesis in *Cymbidium* flowers, we carried out metabolite and gene expression analyses using *Cymbidium* flowers grown under different conditions. *Cymbidium* Sazanami 'Champion' with floral buds at stage S2 were grown at two different temperatures, namely low (20°C/15°C) or high (30°C/25°C). The low-temperature conditions in this study represented temperatures representative of those at which *Cymbidium* blooms in Japan. As shown in Fig. 6, the tepals of *Cymbidium* plants grown at high temperatures (B) were paler than those grown under low-temperature conditions (A). The anthocyanin concentration in tepals grown at

a high temperature decreased to 42.8% of that detected at a low temperature (Fig. 6C). However, no significant difference was observed in the anthocyanin concentration in either the labellum or column between high- and low-temperature conditions. Anthocyanin composition was also different between low- and high-temperature grown plants, with cyanidin 3-malonylglucoside (Cy3MG) concentration being reduced in the three floral organs (Fig. 6C). On the other hand, the flavonol concentrations in the tepals and columns were not affected by the growth temperature, although a significantly ($P < 0.05$) lower flavonol concentration was observed in the labellum grown under high-temperature conditions (Fig. 6D). These results show that anthocyanin concentration decreased in an organ-specific manner, i.e., only in tepals, when *Cymbidium* flowers were exposed to high temperatures.

We also investigated the expression of anthocyanin biosynthesis structural genes in the tepals and labella of flowering plants grown under different temperatures (Fig. 7). High expression levels of *FLS* were detected in the tepals and columns before the temperature treatment started (S2), following which there was no significant decrease in the *FLS* expression levels in either the tepals or labella grown under low- or high-temperature conditions (Fig. 7). This result correlated with changes in the flavonol concentration levels under both temperature conditions. The expression levels of anthocyanin biosynthesis genes, including *CyDFR* and *CyANS*, increased when *Cymbidium* was grown to stage S3 under low-temperature conditions, compared with the expression levels occurring pre-treatment at stage 2 (Fig. 7). However, the expression levels of *CyDFR* and *CyANS* did not increase under high-temperature conditions (Fig. 7). Similarly, the elevated expression of *CyMYB1* and *CybHLH2* observed under low-temperature conditions was not detected under high-temperature conditions in the tepals (Fig. 7). In the labellum of *Cymbidium* flowers grown under the high-temperature

conditions, the expression levels of *CyMYB1*, *CybHLH2*, *CyDFR*, and *CyANS* were suppressed compared with the labellum of flowers grown under low-temperature conditions. However, their transcript abundance in the labellum was higher than that in the tepal under high-temperature conditions. These results indicate that the expression of the regulatory genes *CyMYB1* and *CybHLH2* and the anthocyanin biosynthesis genes *CyDFR* and *CyANS* were suppressed at high temperatures, resulting in the reduced anthocyanin accumulation observed in the tepal organs (Fig. 6).

4. Discussion

Cymbidium flowers exhibited different temporal profiles of anthocyanin accumulation among the tepal, labellum, and column organs (Figs. 1A and 1C). The anthocyanin concentration in all floral organs increased as the *Cymbidium* flowers developed. In tepals, anthocyanin accumulation increased 16.6-fold from flower development S1 to S4 (Fig. 1C), whereas in labella, anthocyanin accumulation increased 5.8-fold during flower development. Anthocyanin accumulation was observed in the entire tepal, whereas it occurred in only the upper part of the labellum organs (Fig. 1A). On the other hand, the base of the column organ started to accumulate anthocyanins at S2. No difference in the flavonol accumulation profiles was observed among the three floral organs (Fig. 1D). Thus, we speculated that anthocyanin accumulation is strictly regulated in an organ-specific manner in *Cymbidium* flowers.

Some anthocyanin biosynthesis-related genes from *Cymbidium* had been reported previously [9, 10]. Wang et al. [10] reported the temporal and spatial expression profiles of some anthocyanin biosynthesis genes, *CHS*, *F3'H*, *DFR*, and *ANS*, in eight *Cymbidium* cultivars with different flower colors and color patterns. However, this paper did not investigate the integrated regulation of anthocyanin biosynthesis genes. The regulatory

mechanism of anthocyanin biosynthesis has been well studied in model plants, including *A. thaliana*, *Z. mays*, *A. majus*, and *P. × hybrida* [3, 4]. The R2R3-MYB and bHLH proteins that regulate anthocyanin biosynthesis have been extensively studied in many floricultural plants, including lily [43, 44], Japanese gentian [11, 45], and *Dendrobium* hybrid [13]. *C. ensifolium*, which is one of the parents used in the breeding of *Cymbidium* hybrids, is the source of several bio-resources including transcriptome [19, 20], proteome [21] and small-RNA transcriptome analyses [18]. However, anthocyanin accumulation is not observed in the *C. ensifolium* floral organs except for the tepals. Therefore, we carried out next-generation sequencing using the red-colored flower of the *Cymbidium* hybrid 'Mystique'. In this study, we were successful in isolating almost all of the regulatory and structural genes involved in anthocyanin biosynthesis from the *Cymbidium* hybrid. Expressed-sequence tag sequencing using next-generation sequencing is important for conducting functional analysis, especially on horticultural plants where genome information is lacking. Next-generation sequencing technology has been utilized to identify several genes related to important floral traits of *Chrysanthemum × morifolium* [22], *Lilium* hybrid [23], and *Paeonia lactiflora* [24].

We isolated genes encoding 15 R2R3-MYB transcription factors from *Cymbidium* hybrid 'Mystique' floral cDNA contigs, with only *CyMYB1* being categorized into a clade belonging to the anthocyanin biosynthesis regulators reported in other orchids (Fig. 2). The deduced amino acid sequence of *CyMYB1* showed strong similarity with that of the anthocyanin biosynthesis-related R2R3-MYB transcription factors from other orchid species, including *Oncidium* OgMYB1 [5, 6], *Dendrobium* DhMYB2 [13], and *Phalaenopsis* PeMYBs [8]. Anthocyanin biosynthesis-related R2R3-MYBs are categorized into two subgroups, *C1* and *AN2*, based on the amino acid sequences [46]. Most *R2R3-MYB* genes that regulate anthocyanin biosynthesis in flowers of eudicot

476 species and monocot *Lilium* species are in the *AN2* subgroup [44, 46]. On the other hand,
477 anthocyanin biosynthesis-related *R2R3-MYB* genes of most monocots, including
478 members of the Poaceae and Orchidaceae, belong to the *C1* subgroup. CyMYB1 was also
479 categorized into the same *C1* subgroup as anthocyanin regulatory factors from other
480 Orchidaceae species (Fig. 2).

481 *Phalaenopsis* spp. has three anthocyanin biosynthesis-related *R2R3-MYB* genes,
482 namely *PeMYB2*, *PeMYB11*, and *PeMYB12* [8]. Although they were grouped together in
483 the same clade, PeMYB2 showed strong activity with respect to anthocyanin biosynthesis,
484 whereas PeMYB11 and PeMYB12 exhibited little activity. In the sepals/petals, PeMYB2,
485 PeMYB11, and PeMYB12 control full-red pigmentation, red spots, and venation patterns,
486 respectively [8]. Moreover, PeMYB11 controls the production of red spots in the callus,
487 and PeMYB12 is the major transcription factor controlling pigmentation in the central
488 lobe of the labellum [8]. *Cymbidium* flowers also exhibit a wide range of intricate
489 anthocyanin pigmentation patterns, including full tepal pigmentation, venation, spots,
490 zones that lack pigmentation, and co-pigmentation (Figs. 1A and 6A) [47]. However, we
491 could not find any R2R3-MYB homologs belonging to the *C1* subgroup except for
492 CyMYB1 from the *Cymbidium* hybrid flower (Fig. 2). It is possible that some *CyMYB1*-
493 like *R2R3-MYB* genes might be isolated from other *Cymbidium* cultivars with spotting or
494 venation patterns. Albert et al. [14] reported that the combination of *C1* (*R2R3-MYB)* and
495 *Lc* (*bHLH*) genes from *Z. mays* could induce anthocyanin pigmentation in the petals of
496 the *Cymbidium* hybrid 'Jung Frau dos Pueblos', which is a commercial white-flowered
497 cultivar. These results implied that *C1* and *Lc* orthologs might regulate anthocyanin
498 biosynthesis in *Cymbidium* flowers. The phylogenetic analysis showed that CybHLH1
499 and CybHLH2 were classified into the same clade as *Z. mays* Lc rather than other orchid
500 bHLHs (Supplementary Fig. S2). These results suggested strongly that anthocyanin

accumulation in the *Cymbidium* flower is regulated by *CyMYB1* and *CybHLH1/2*, which are maize *C1* and *Lc* orthologs, respectively. Moreover, yeast two-hybrid analysis showed that CyMYB1 could interact with either CybHLH1 or CybHLH2 (Fig. 3). Therefore, this result also implied that the complex of CyMYB1 and CybHLH1/2 regulates anthocyanin biosynthesis in the floral organs of *Cymbidium*.

The temporal and spatial profiles of the *CyMYB1* transcripts correlated closely with the profile of anthocyanin accumulation in the tepals (Fig. 1C and 4). On the other hand, neither *CybHLH1* nor *CybHLH2* showed such a dynamic variation in transcript abundance, which reflected the observed changes in anthocyanin and flavonoid accumulation (Fig. 1C and 4). Therefore, we speculated that *CyMYB1* is a key regulatory gene for anthocyanin biosynthesis in *Cymbidium* floral organs. In the kernel of *Z. mays*, MYB (C1/Pl) and bHLH (R1/B1) interact and activate the anthocyanin biosynthesis genes *CHS*, *CHI*, *F3H*, *DFR*, *ANS*, and *3GT* as a single unit [48]. In proanthocyanidin biosynthesis in *Arabidopsis* seeds, TT2, TT8, and TTG1 are involved in the MYB-bHLH-WDR complex, and they control the expression of the late biosynthesis genes, including *DFR*, *ANS*, *3GT*, leucoanthocyanidin reductase, and anthocyanidin reductase [48]. In anthocyanin synthesis in grapes, transcription of the *3GT* gene alone was regulated by two *MYB* genes, *VvMYBA1* and *VvMYBA2* [49, 50]. In a *Dendrobium* hybrid, *DhMYB2* and *DhbHLH1* were synchronously expressed during petal development, and directly activated the transcription of *DhF3H*, *DhDFR*, and *DhANS* [13]. In an *Oncidium* hybrid, *OgMYB1* activated the transcription of the *OgCHI* and *OgDFR* genes, resulting in anthocyanin accumulation in normally unpigmented floral lip tissues [5, 6]. In the present study, of 12 anthocyanin and flavonol biosynthesis genes, the expression profiles of the *CyCHS*, *CyF3H*, *CyF3'H2*, *CyDFR*, *CyANS* and *CyMalT* genes were similar to that of *CyMYB1* in tepals (Figs. 4 and 5). In the labella, the temporal expression profiles of

526 *CyDFR, CyANS*, and *CyMalT* were also correlated with that of *CyMYB1* (Figs. 4 and 5).
527 However, the expression profiles of structural genes encoding anthocyanin
528 glycosyltransferases, including *Cy3GT* and *Cy3RT*, were not correlated with that of
529 *CyMYB1* in the tepal or labellum organs (Fig. 4). Therefore, the expression of genes
530 encoding these anthocyanin modification enzymes might not be controlled directly by
531 *CyMYB1*. However, since both *Cy3RT* and *CyMalT* were candidate genes found among
532 the *Cymbidium* floral cDNA contigs (Supplementary Figs. S6 and S7), it would be
533 necessary to carry out further functional analysis on these genes. These results imply that
534 CyMYB1 interacted with either CybHLH1 or CybHLH2 and activated the transcription
535 of *CyCHS, CyF3H,* and *CyF3'H* in the tepals as well as of *CyDFR, CyANS and CyMalT*
536 in tepals and labella during flower development. However, we were not successful in
537 activating anthocyanin biosynthesis by transient expression of *CyMYB1* in several organs
538 of *Cymbidium* (data not shown). Moreover, no different observations of flower colors
539 were made when *CyMYB1* was overexpressed in transgenic tobacco plants (data not
540 shown). Therefore, we would remain to further study to reveal *CyMYB1* function in
541 *Cymbidium* flowers.

542 The growth temperature is one of the main environmental factors affecting
543 anthocyanin accumulation in plant tissues [29, 35]. Generally, low temperature increases
544 anthocyanin concentration, whereas elevated temperature decreases it. Of the *Cymbidium*
545 floral organs, the tepals showed significantly lower anthocyanin concentrations under
546 high temperatures (Fig. 6C). However, no significant reduction in the concentration of
547 anthocyanins in the labellum and column organs at high temperature was observed (Fig.
548 6C). Thus, anthocyanin accumulation in the tepal organ showed a different response at
549 high temperature than that in the labellum organs, which was the other petal-like floral
550 organ. On the other hand, no marked changes in flavonol concentrations were observed

551 in any of the floral organs (Fig. 6D). This result suggested that the accumulation of
552 flavonols had been completed by stage 2, at which the plant material was moved to the
553 high growth temperature, since flavonols are synthesized during the early floral
554 developmental stage (Fig. 1D). In rose (*Rosa hybrida*), the expression levels of *CHS* and
555 *DFR* decreased by 50% after heat treatment (39°C/18°C), suggesting that the decreased
556 anthocyanin concentration was due, at least in part, to reduced transcription of these genes
557 [29, 35]. In the Oriental hybrid lily "Marrero," elevated temperature caused low
558 coloration in the tepal organs at stages 2 and 3, during which increasing concentrations
559 of anthocyanins would usually accumulate [30]. It has also been reported that anthocyanin
560 accumulation in petunia petals was increased by low-temperature incubation [25, 26]. The
561 expression levels in lily of the *LhMYB12*, *CHS*, *F3H*, and *DFR* genes was suppressed
562 under a high-temperature treatment (30°C/25°C) compared with a low-temperature
563 treatment (20°C/15°C) [30]. Therefore, the reduced transcription of *LhMYB12*, which is
564 a key anthocyanin biosynthesis regulatory gene, caused by high temperature, was
565 responsible for the reduced anthocyanin accumulation in lily tepals under these conditions
566 [30]. In the present study, when *Cymbidium* Sazanami 'Champion' was exposed to high
567 temperatures, a marked decrease in the expressions of *CyMYB1*, *CyDFR*, and *CyANS* was
568 detected in the tepal organs (Fig. 7). The expressions of these three genes in the labellum
569 were also suppressed under high temperatures, but they were higher than those in the
570 tepals. Therefore, tepal organ-specific anthocyanin suppression was thought to result
571 from the suppression of *CyMYB1* at high temperatures. In addition, this finding strongly
572 suggests that *CyMYB1* is directly regulate the transcription of the two late anthocyanin
573 biosynthesis genes, *CyDFR* and *CyANS*, in *Cymbidium* floral organs.
574 Thus, we demonstrated that organ-specific and temperature-dependent anthocyanin
575 pigmentation could be regulated by a *CyMYB1* in *Cymbidium* hybrid flowers, and the

CyMYB1 interacts with CybHLH1/2, with this complex activating the transcription of *CyDFR* and *CyANS*. Moreover, we demonstrated that the reduced anthocyanin concentration in the tepals developing at high temperatures was associated with reduced expression of *CyMYB1*.

Declaration of interest

None.

Author's contribution

T. Nakatsuka, T. Suzuki, H. Dohra, and H. Ohno conceived and designed the experiments. T. Nakatsuka, T. Suzuki, H. Dohra, K. Harada and Y. Kobayashi carried out the experiments. T. Nakatsuka wrote the paper. T. Suzuki, H. Dohra and H. Ohno edited the manuscripts. All authors reviewed the results and approved the final version of the manuscript.

Finding

This study was supported by KAKENHI Grant Number 26450032, Japan Society for Promotion of Science, and by the Program to Disseminate Tenure Tracking System, Japan Science and Technology Agency.

Acknowledgements

We thank Dr. Fumi Tatsuzawa, Iwate University, to help flavonoid analysis.

References

[1] F. Tatsuzawa, N. Saito, M. Yokoi, Anthocyanins in the flowers of *Cymbidium*,

601 Lindleyana, 11 (1996) 214-219.
602 [2] J. Arditti, Fundamentals of Orchid Biology, John Wiley and Sons, New York, 1992.
603 [3] K.M. Davies, Modifying anthocyanin production in flowers, in: K. Gould, K. Davies,
604 C. Winefield (Eds.) Anthocyanins Biosynthesis, Functions, and Applications,
605 Springer, New York, 2009, pp. 49-83.
606 [4] J. Mol, E. Grotewold, R. Koes, How genes paint flowers and seeds, Trend Plant Sci,
607 3 (1998) 212-217.
608 [5] C.Y. Chiou, K.W. Yeh, Differential expression of *MYB* gene (*OgMYB1*) determines
609 color patterning in floral tissue of *Oncidium* Gower Ramsey, Plant Mol Biol, 66
610 (2008) 379-388.
611 [6] C.Y. Chiou, K.W. Yeh, Coloration and color patterning in floral tissues of *Oncidium*
612 Grwer Ramsey, in: W.H. Chen, H.H. Chen (Eds.) Orchid Biotechnology II, World
613 Scientific, Singapore, 2011, pp. 101-115.
614 [7] A.D. Hieber, R.G. Mudalige-Jayawickrama, A.R. Kuehnle, Color genes in the orchid
615 *Oncidium* Gower Ramsey: identification, expression, and potential genetic
616 instability in an interspecific cross, Planta, 223 (2006) 521-531.
617 [8] C.C. Hsu, Y.Y. Chen, W.C. Tsai, W.H. Chen, H.H. Chen, Three R2R3-MYB
618 transcription factors regulate distinct floral pigmentation patterning in *Phalaenopsis*
619 spp, Plant Physiol, 168 (2015) 175-191.
620 [9] E.T. Johnson, H. Yi, B. Shin, B.J. Oh, H. Cheong, G. Choi, *Cymbidium hybrida*
621 dihydroflavonol 4-reductase does not efficiently reduce dihydrokaempferol to
622 produce orange pelargonidin-type anthocyanins, Plant J, 19 (1999) 81-85.
623 [10] L. Wang, N.W. Albert, H. Zhang, S. Arathoon, M.R. Boase, H. Ngo, K.E. Schwinn,
624 K.M. Davies, D.H. Lewis, Temporal and spatial regulation of anthocyanin
625 biosynthesis provide diverse flower colour intensities and patterning in *Cymbidium*

626 orchid, Planta, 240 (2014) 983-1002.
627 [11] T. Nakatsuka, N. Sasaki, M. Nishihara, Transcriptional regulators of flavonoid
628 biosynthesis and their application to flower color modification in Japanese gentians,
629 Plant Biotechnol, 31 (2014) 389-399.
630 [12] W. Xu, C. Dubos, L. Lepiniec, Transcriptional control of flavonoid biosynthesis by
631 MYB-bHLH-WDR complexes, Trends Plant Sci, 20 (2015) 176-185.
632 [13] C. Li, J. Qiu, L. Ding, M. Huang, S. Huang, G. Yang, J. Yin, Anthocyanin
633 biosynthesis regulation of *DhMYB2* and *DhbHLH1* in *Dendrobium* hybrid petals,
634 Plant Physiol Biochem, 112 (2017) 335-345.
635 [14] N.W. Albert, S. Arathoon, V.E. Collette, K.E. Schwinn, P.E. Jameson, D.H. Lewis,
636 H. Zhang, K.M. Davies, Activation of anthocyanin synthesis in *Cymbidium* orchids:
637 variability between known regulators, Plant Cell Tiss Organ Cult, 100 (2010) 355-
638 360.
639 [15] C.H. Fu, Y.W. Chen, Y.Y. Hsiao, Z.J. Pan, Z.J. Liu, Y.M. Huang, W.C. Tsai, H.H.
640 Chen, OrchidBase: a collection of sequences of the transcriptome derived from
641 orchids, Plant Cell Physiol, 52 (2011) 238-243.
642 [16] W.C. Tsai, C.H. Fu, Y.Y. Hsiao, Y.M. Huang, L.J. Chen, M. Wang, Z.J. Liu, H.H.
643 Chen, OrchidBase 2.0: comprehensive collection of Orchidaceae floral
644 transcriptomes, Plant Cell Physiol, 54 (2013) e7.
645 [17] J. Cai, X. Liu, K. Vanneste, S. Proost, W.C. Tsai, K.W. Liu, L.J. Chen, Y. He, Q. Xu,
646 C. Bian, Z. Zheng, F. Sun, W. Liu, Y.Y. Hsiao, Z.J. Pan, C.C. Hsu, Y.P. Yang, Y.C.
647 Hsu, Y.C. Chuang, A. Dievart, J.F. Dufayard, X. Xu, J.Y. Wang, J. Wang, X.J. Xiao,
648 X.M. Zhao, R. Du, G.Q. Zhang, M. Wang, Y.Y. Su, G.C. Xie, G.H. Liu, L.Q. Li, L.Q.
649 Huang, Y.B. Luo, H.H. Chen, Y. Van de Peer, Z.J. Liu, The genome sequence of the
650 orchid *Phalaenopsis equestris*, Nat Genet, 47 (2015) 65-72.

[18] X. Li, F. Jin, L. Jin, A. Jackson, X. Ma, X. Shu, D. Wu, G. Jin, Characterization and comparative profiling of the small RNA transcriptomes in two phases of flowering in *Cymbidium ensifolium*, BMC Genomics, 16 (2015) 622.

[19] X. Li, J. Luo, T. Yan, L. Xiang, F. Jin, D. Qin, C. Sun, M. Xie, Deep sequencing-based analysis of the *Cymbidium ensifolium* floral transcriptome, PLoS One, 8 (2013) e85480.

[20] F. Yang, G. Zhu, Digital gene expression analysis based on *de novo* transcriptome assembly reveals new genes associated with floral organ differentiation of the orchid plant *Cymbidium ensifolium*, PLoS One, 10 (2015) e0142434.

[21] X. Li, W. Xu, M.R. Chowdhury, F. Jin, Comparative proteomic analysis of labellum and inner lateral petals in *Cymbidium ensifolium* flowers, Int J Mol Sci, 15 (2014) 19877-19897.

[22] K. Sasaki, N. Mitsuda, K. Nashima, K. Kishimoto, Y. Katayose, H. Kanamori, A. Ohmiya, Generation of expressed sequence tags for discovery of genes responsible for floral traits of *Chrysanthemum morifolium* by next-generation sequencing technology, BMC Genomics, 18 (2017) 683.

[23] K. Suzuki, T. Suzuki, T. Nakatsuka, H. Dohra, M. Yamagishi, K. Matsuyama, H. Matsuura, RNA-seq-based evaluation of bicolor tepal pigmentation in Asiatic hybrid lilies (*Lilium* spp.), BMC Genomics, 17 (2016) 611.

[24] D. Zhao, Y. Jiang, C. Ning, J. Meng, S. Lin, W. Ding, J. Tao, Transcriptome sequencing of a chimaera reveals coordinated expression of anthocyanin biosynthetic genes mediating yellow formation in herbaceous peony (*Paeonia lactiflora* Pall.), BMC Genomics, 15 (2014) 689.

[25] M. Shvarts, A. Borochov, D. Weiss, Low temperature enhances petunia flower pigmentation and induces chalcone synthase gene expression, Physiol Plant, 99

(1997) 67-72.

[26] M. Shvarts, D. Weiss, A. Borochov, Temperature effects on growth, pigmentation and post-harvest longevity of petunia flowers, Sci Hort, 69 (1997) 217-227.

[27] K. Nozaki, T. Takamura, S. Fukai, Effects of high temperature on flower colour and anthocyanin content in pink flower genotypes of greenhouse chrysanthemum (*Chrysanthemum morifolium* Ramat.), J Hort Sci Biotechnol, 81 (2006) 728-734.

[28] L. Shaked-Sachray, D. Weiss, M. Reuveni, A. Nissim-Levi, M. Oren-Shamir, Increased anthocyanin accumulation in aster flowers at elevated temperatures due to magnesium treatment, Physiol Plant, 114 (2002) 559-565.

[29] G. Dela, E. Or, R. Ovadia, A. Nissim-Levi, D. Weiss, M. Oren-Shamir, Changes in anthocyanin concentration and composition in 'Jaguar' rose flowers due to transient high-temperature conditions, Plant Sci, 2003 (2003) 333-340.

[30] Y.S. Lai, M. Yamagishi, T. Suzuki, Pigment accumulation and transcription of *LhMYB12* and anthocyanin biosynthesis genes during flower development in the Asiatic hybrid lily (*Lilium* spp.), Plant Sci, 132 (2011) 59-65.

[31] X.B. Xie, S. Li, R.F. Zhang, J. Zhao, Y.C. Chen, Q. Zhao, Y.X. Yao, C.X. You, X.S. Zhang, Y.J. Hao, The bHLH transcription factor *MdbHLH3* promotes anthocyanin accumulation and fruit colouration in response to low temperature in apples, Plant Cell Environ, 35 (2012) 1884-1897.

[32] K. Mori, N. Goto-Yamamoto, M. Kitayama, K. Hashizume, Loss of anthocyanins in red-wine grape under high temperature, J Exp Bot, 58 (2007) 1935-1945.

[33] A. Leyva, J.A. Jarillo, J. Salinas, J.M. Martinez-Zapater, Low temperature induces the accumulation of phenylalanine ammonia-lyase and chalcone synthase mRNAs of *Arabidopsis thaliana* in a light-dependent manner, Plant Physiol, 108 (1995) 39-46.

701 [34] P.J. Christie, M.R. Alfenito, V. Walbot, Impact of low-temperature stress on general
702 phenylpropanoid and anthocyanin pathways: Enhancement of transcript abundance
703 and anthocyanin pigmentation in maize seedlings, Planta, 194 (1994) 541-549.
704 [35] D. Weiss, Regulation of flower pigmentation and growth: Multiple signaling
705 pathways control anthocyanin synthesis in expanding petals, Physiol Plant, 110
706 (2000) 152-157.
707 [36] M. Martin, Cutadapt removes adapter sequences from high-throughput sequencing
708 reads, EMBnet J, 17 (2011) 10-12.
709 [37] M.G. Grabherr, B.J. Haas, M. Yassour, J.Z. Levin, D.A. Thompson, I. Amit, X.
710 Adiconis, L. Fan, R. Raychowdhury, Q. Zeng, Z. Chen, E. Mauceli, N. Hacohen, A.
711 Gnirke, N. Rhind, F. di Palma, B.W. Birren, C. Nusbaum, K. Lindblad-Toh, N.
712 Friedman, A. Regev, Full-length transcriptome assembly from RNA-seq data
713 without a reference genome, Nat Biotechnol, 29 (2011) 644-652.
714 [38] S. Gotz, J.M. Garcia-Gomez, J. Terol, T.D. Williams, S.H. Nagaraj, M.J. Nueda, M.
715 Robles, M. Talon, J. Dopazo, A. Conesa, High-throughput functional annotation and
716 data mining with the Blast2GO suite, Nucleic Acids Res, 36 (2008) 3420-3435.
717 [39] J.D. Thompson, D.G. Higgins, T.J. Gibson, Improved sensitivity of profile searches
718 through the use of sequence weights and gap excision, Comput Appl Biosci, 10
719 (1994) 19-29.
720 [40] K. Tamura, G. Stecher, D. Peterson, A. Filipski, S. Kumar, MEGA6: Molecular
721 Evolutionary Genetics Analysis version 6.0, Mol Biol Evol, 30 (2013) 2725-2729.
722 [41] I.M. Zimmermann, M.A. Heim, B. Weisshaar, J.F. Uhrig, Comprehensive
723 identification of *Arabidopsis thaliana* MYB transcription factors interacting with
724 R/B-like BHLH proteins, Plant J, 40 (2004) 22-34.
725 [42] A. Nakatsuka, M. Yamagishi, M. Nakano, K. Tasaki, N. Kobayashi, Light-induced

726 expression of basic helix-loop-helix genes involved in anthocyanin biosynthesis in
727 flowers and leaves of Asiatic hybrid lily, Sci Hortic, 121 (2009) 84-91.
728 [43] M. Yamagishi, How genes paint lily flowers: Regulation of colouration and
729 pigmentation patterning, Sci Hort, 163 (2013) 27-36.
730 [44] M. Yamagishi, Y. Shimoyamada, T. Nakatsuka, K. Masuda, Two *R2R3-MYB* genes,
731 homologs of petunia *AN2*, regulate anthocyanin biosyntheses in flower tepals, tepal
732 spots and leaves of asiatic hybrid lily, Plant Cell Physiol, 51 (2010) 463-474.
733 [45] T. Nakatsuka, K.S. Haruta, C. Pitaksutheepong, Y. Abe, Y. Kakizaki, K. Yamamoto,
734 N. Shimada, S. Yamamura, M. Nishihara, Identification and characterization of
735 R2R3-MYB and bHLH transcription factors regulating anthocyanin biosynthesis in
736 gentian flowers, Plant Cell Physiol, 49 (2008) 1818-1829.
737 [46] A.C. Allan, R.P. Hellens, W.A. Laing, MYB transcription factors that colour our fruit,
738 Trends Plant Sci, 13 (2008) 99-102.
739 [47] N. Albert, K. Davies, K. Schwinn, Gene regulation networks generate diverse
740 pigmentation patterns in plants, Plant Signal Behav, 9 (2014) 962-980.
741 [48] K. Petroni, C. Tonelli, Recent advances on the regulation of anthocyanin synthesis
742 in reproductive organs, Plant Sci, 181 (2011) 219-229.
743 [49] P.K. Boss, C. Davies, S.P. Robinson, Analysis of the expression of anthocyanin
744 pathway genes in developing *Vitis vinifera* L. Mist. Shiraz grape berries and the
745 Implications for pathway regulation, Plant Physiol, 111 (1996) 1059-1066.
746 [50] M.C. Cutanda-Perez, A. Ageorges, C. Gomez, S. Vialet, N. Terrier, C. Romieu, L.
747 Torregrosa, Ectopic expression of *VlmybA1* in grapevine activates a narrow set of
748 genes involved in anthocyanin synthesis and transport, Plant Mol Biol, 69 (2009)
749 633-648.
750 [51] A.R. Rinaldo, E. Cavallini, Y. Jia, S.M. Moss, D.A. McDavid, L.C. Hooper, S.P.

Robinson, G.B. Tornielli, S. Zenoni, C.M. Ford, P.K. Boss, A.R. Walker, A grapevine anthocyanin acyltransferase, transcriptionally regulated by *VvMYBA*, can produce most acylated anthocyanins present in grape skins, Plant Physiol, 169 (2015) 1897-1916.

Figure legends

Figure 1. Temporal and spatial accumulation patterns of flavonoids in *Cymbidium* 'Mystique' floral organs.

A. The different organs of the orchid flowers are given in white letters as follows: S, petal-like sepal; P, lateral petal; L, labellum; C, column. Tepal is a general term for both petal-like sepals and lateral petals. Bar = 1 cm.

B. Flower developmental stages (Stages (S) 1 to 4) as described in the Materials and methods section. Bar = 1 cm.

C. Anthocyanin accumulation profiles of different floral organs of *Cymbidium* 'Mystique' during flower development. Value and error bars indicate the mean ± standard error (n = 5). Cy3G, cyanidin 3-*O*-glucoside; Cy3G, cyanidin 3-*O*-rutinoside; Pe3R, peonidin 3-*O*-rutinoside; Cy3MG, cyanidin 3-malonylglucoside.

D. Flavonol accumulation profiles of different floral organs of *Cymbidium* 'Mystique' during flower development. The flavonol concentration was determined from the peak area detected at 360 nm. Value and error bars indicate the mean ± standard error (n = 5).

Figure 2. Phylogenetic tree inferred from the amino acid sequences of the R2R3 region of CyMYBs with R2R3-MYB from other species.

This phylogenetic tree was constructed by the neighbor-joining method with 1,000 bootstrapping data sets. R2R3-MYB name and GenBank accession number are indicated

as follows: *Antirrhinum majus* MIXTA (Q38739), MYB305(P81391), PHAN (O65366), ROSEA1 (ABB83826), ROSEA2 (ABB8327), and VENOSA (ABB83828); *Arabidopsis thaliana* AS1 (O80931), ATR1 (O64399), GL1 (P27900), MYB2 (Q39028), MYB12 (O22264), PAP1 (Q9FE25), PAP2 (Q9ZTC3), PCMYB1 (Q9S7G7), TT2 (Q9FJA2), and WER (Q9SEI0); *Cymbidium* hybrid CyMYB1 to CyMYB16 (in this study); *Dendrobium* hybrid MYB1 (K7ZBK1) and MYB2 (A0A1S6JNE7); *Gentiana triflora* MYB3 (A9ZMI4), MYBP3 (L0N1P2), and MYBP4 (A9ZMI5); *Hordeum vulgare* GAMYB (Q96464); *Lilium* hybrid MYB6 (D4QF65) and MYB12 (D4QF64); *Nicotiana tabacum* MYBA1 (Q948S6); *Oncidium* hybrid MYB1 (A7KTI5); *Phalaenopsis* ssp. MYB2 (A0A096ZX46), MYB11 (A0A096ZX39), and MYB12 (A0A096ZX55); *Petunia hybrida* AN2 (Q9M72) and MYBPH3 (Q02992); *Vitis vinifera* MYBA1-1 (Q8L5P3); *Zea mays* C1 (P10290), P (P27898), Pl (O22450) and RS2 (Q9S7B2). Scale bar represents 0.1 substitution per site.

Figure 3. Protein–protein interaction between CyMYB1 and CybHLHs

The CyMYB1, CybHLH1, and CybHLH2 proteins were fused to the GAL4 DNA-binding domain or to the GAL4 activation domain. pGBKT7 and pGADT7 are the negative controls for bait and prey, respectively. Yeast was grown on double-selection medium (−Leu, −Trp) and quadruple-selection medium (−Leu, −Trp, −His, −Ade) supplemented with 15 mM 3-AT at 30°C for 2 to 3 days.

Figure 4. Relative expression levels of anthocyanin biosynthesis regulatory genes in each floral organ of *Cymbidium* hybrid 'Mystique' during flower development

Value and error bars are the mean ± standard error (n = 6).

Figure 5. Relative expression levels of anthocyanin and flavonol biosynthesis structural genes in each floral organ of *Cymbidium* hybrid 'Mystique' during flower development

Value and error bars are the mean ± standard error (n = 6).

Figure 6. Effect of growth temperature on flower pigmentation of *Cymbidium* Sazanami 'Champion'

A) Cymbidium flowers grown at 20°C/15°C (L). **B)** Cymbidium flowers grown at 30°C/25°C (H). Bar = 1 cm.

C) Anthocyanin concentration profiles of each floral organ of *Cymbidium* Sazanami 'Champion' grown at different temperatures. Value and error bars indicate the mean ± standard error (n = 5). Cy3G, cyanidin 3-*O*-glucoside; Cy3G, cyanidin 3-*O*-rutinoside; Pe3R, peonidin 3-*O*-rutinoside; Cy3MG, cyanidin 3-malonylglucoside.

D) Flavonol concentration profiles of each floral organ of *Cymbidium* Sazanami 'Champion' grown at different temperatures. Flavonol concentrations were determined from the peak area detected at 360 nm. Asterisks indicate statistically significant difference between the 20°C/15°C (L) and 30°C/25°C (H) treatments using the Student's *t*-test (**, $P < 0.01$).

Figure 7. Effect of growth temperature on the expression levels of anthocyanin biosynthesis-related genes of *Cymbidium* Sazanami 'Champion'

Relative expression levels of *Cymbidium* anthocyanin biosynthesis regulatory and enzymatic genes in each floral organ of *Cymbidium* Sazanami 'Champion' grown at different temperatures. S2 is a sample at stage 2 before temperature treatment. L and H are samples collected at stage 4 after they were grown at 20°C/15°C and 30°C/25°C,

826 respectively. Value and error bars are the mean ± standard error (n = 6).

827

828 **Supplementary Figure S1. Regulation of the anthocyanin biosynthesis pathway by**
829 **the transcription factor CyMYB1**

830 CHS, chalcone synthase; CHI, chalcone isomerase; F3H, flavanone 3-hydroxylase;
831 F3′H, flavonoid 3′-hydroxylase; DFR, dihydroflavonol 4-reductase; ANS, anthocyanidin
832 synthase; 3GT, anthocyanidin 3-*O*-glucosyltransferase; 3RT, UDP-rhamnose:
833 anthocyanin 3-*O*-glucoside-rhamnosyltransferase; MalT, anthocyanin: malonyl-CoA
834 acyltransferase; FLS, flavonol synthase. Blue characterized genes were identified in
835 current study. This study indicated that *CyMYB1* was key regulatory gene for tepal- and
836 temperature-dependent anthocyanin accumulation to activate transcription of *CyDFR* and
837 *CyANS* in *Cymbidium*.

838

839 **Supplementary Figure S2. Phylogenetic tree inferred from amino acid sequences of**
840 ***bHLH* genes from *Cymbidium* and other species**

841 This phylogenetic tree was constructed by the neighbor-joining method with 1,000
842 bootstrapping data sets. bHLH name and GenBank accession number are indicated as
843 follows: *Antirrhinum majus* delila (Q38736), *Arabidopsis thaliana* MYC1 (Q8W2F1),
844 EGL1 (Q9CAD0), GL3 (Q9FN69), and TT8 (Q9FT81), *Cymbidium* hybrid bHLH1 and
845 bHLH2 (in this study), *Dendrobium* hybrid (A0A1S6JNE8), *Gentiana triflora* (B7XEI1|),
846 *Gerbera hybrida* (O82686), *Ipomoea nil* bHLH1 (Q1JV08), bHLH2 (Q1JV07), and
847 bHLH3 (Q1JV06), *Lilium* hybrid (Q401N5), *Oryza sativa* Ra (Q40643) and Rc (Q2I7J3),
848 *Perilla frutescens F3G1*(Q852P3) and MYC-RP (Q9ZQS4), *Petunia hybrida* AN1
849 (Q9FEA1), JAF13 (O64908), *Phalaenopsis* spp. (A0A096ZX60), and *Zea mays* In1
850 (Q41875) and Lc (P13526). Scale bar represents 0.1 substitution per site.

Supplementary Figure S3. Phylogenetic tree inferred from the amino acid sequences of CHI from *Cymbidium* and other species

This phylogenetic tree was constructed by the neighbor-joining method with 1,000 bootstrapping data sets. CHI name and GenBank accession number are indicated as follows: *Allium cepa* (Q6QHK0), *Arabidopsis thaliana* (P41088), *Camellia sinensis* (Q45QI7), *Chrysanthemum morifolium* CHI1 (A1E260) and CHI2 (A1E261), *Citrus sinensis* (Q9ZWR1), *Cymbidium* hybrid CHI1 and CHI2 (in this study), *Dendrobium* hybrid (V9PCX1), *Dianthus caryophyllus* (Q43754), *Elaeagnus umbellata* (O65333), *Eustoma exaltatum* (Q6BEH3), *Gentiana triflora* CHI1 (Q565D8) and CHI2 (unpublished data), *Glycine max* CHI1 (B2CM87), CHI2 (B2CM88) and CHI3 (A7ISP6), *Ipomoea nil* EFP (X5IGL5), *Ipomoea purpurea* (O22604), *Lotus japonicus* CHI1 (I3SU15), CHI2 (Q8H0G1), and CHI3 (I3SKD9), *Medicago sativa* (U5TRY3), *Nicotiana tabacum* (Q33DL3), *Oncidium* hybrid (A7KTI4), *Petunia hybrida* CHIA (P11650), CHIB (P11651), CHIC (Q9M5B3), and EFP (D7US50), *Phalaenopsis equestris* (A0A096ZX25), *Phaseolus vulgaris* (P14298), *Raphanus sativus* (O22651), *Torenia hybrida* CHI4B (D7US52) and EFP (D7US51), *Tricyrtis* spp. (W6JMJ6), *Tulipa fosteriana* (A0A088CB22), *Vitis vinifera* (P51117), and *Zea mays* (Q08704). Scale bar represents 0.1 substitution per site.

Supplementary Figure S4. Phylogenetic tree inferred from the amino acid sequences of F3H, ANS, and FLS from *Cymbidium* and other species

This phylogenetic tree was constructed by the neighbor-joining method with 1,000 bootstrapping data sets.

F3H name and GenBank accession number are indicated as follows: *Actinidia*

chinensis (B8YLW1), *Cymbidium* hybrid (this study), *Gentiana triflora* (Q59I70), *Lilium* hybrid (I7HDC7), *Lilium speciosum* (Q2L6K2), *Perilla frutescens* (O04112), *Persea americana* (Q40754), *Petunia hybrida* (Q07353), and *Tulipa fosteriana* (M9TGR0)

ANS name and GenBank accession number are indicated as follows: *Cymbidium* hybrid (this study, A0A088G9H7), *Iris hollandica* (A5HUP4), *Gentiana triflora* (Q59I71), *Lilium* hybrid (I7H3Z0), *Petunia hybrida* (P51092), *Pyrus communis* (P51091), *Torenia fournieri* (Q9AYT0), and *Tulipa gesneriana* (C7G0X5).

FLS name and GenBank accession number are indicated as follows: *Allium cepa* (Q84TM1), *Citrus unshiu* (Q9ZWQ9), *Cymbidium* hybrid (this study, and A0A088G4R1), *Dendrobium* hybrid (V9PCW6), *Eustoma exaltatum* (Q9M547), *Gentiana triflora* (F1SZA2), *Petunia hybrida* (Q07512), and *Tricyrtis* spp. (A0A0U5AET0). Scale bar represents 0.1 substitution per site.

Supplementary Figure S5. Phylogenetic tree and alignment inferred from the amino acid sequences of F3′H predicted by *Cymbidium* hybrid and other species.

A) This phylogenetic tree was constructed by the neighbor-joining method with 1,000 bootstrapping data sets. *F3′H* name and GenBank accession number are indicated as follows: *Cymbidium* hybrid CyF3′H1 and CyF3′H2 (this study), *Epimedium sagittatum* (D5M8Q3), *Gentiana triflora* (Q59I68), *Gerbera hybrida* (Q38L00), *Lilium* hybrid F3′H1 (I7H3Y9), *Perilla frutescens* (Q93XJ2), *Petunia hybrida* Ht1 (Q9SBQ9), *Phalaenopsis* hybrid F3′5′H (Q3YAF0), *Torenia* hybrida (Q8S9C7), *Tricyrtis hirta* (B9A9Y6), *Tulipa fosteriana* (M9TH21), and *Vitis vinifera* (Q3C212). Scale bar represents 0.1 substitution per site.

B) Alignment of the full-length deduced amino acid sequences of CyF3′H1, CyF3′H2, and ChF3′H (KM186178) using ClustalW (Thompson et al., 1994). Red characters of

amino acid sequences show tree consensus domains, including proline rich region (PPxP), threonine-containing binding pocket for oxygen molecules required in catalysis (A/G)Gx(D/E)T(T/S), and the heme-binding domain (FxxGxRxCxG).

Supplementary Figure S6. Phylogenetic tree inferred from the amino acid sequences of GT from *Cymbidium* hybrid and other species.

This phylogenetic tree was constructed by the neighbor-joining method with 1,000 bootstrapping data sets. GT name and GenBank accession number are indicated as follows: *Antirrhinum majus* chalcone 4′GT (Q33DV3); *Arabidopsis* At4g14090 (5GT, W8Q6K8), *Vigna mungo* 3GaT (Q9ZWS2), *Celosia cristata* cDOPA5GT (Q59J80), *Cleretum bellidiforme* cDOPA5GT, *Cymbidium* hybrid 3GT and 3RT (in this study), *Eustoma exaltatum* 5GT (A4F1Q3), *Gentiana triflora* 3GT (Q96493), 3'GT (Q8H0F2), and 5GT (B2NID7), *Ipomoea purpurea* 3GGT (Q53UH5), *Iris hollandica* 5GT (Q767C8), *Mirabilis jalapa* cDOPA5GT (Q59J81), *Perilla frutescens* 5GT (Q9ZR26), *Petunia hybrida* 3GT (Q9SBQ3), 3RT (Q43716), and 5GT (Q9SBQ2), *Rosa hybrida* 5,3-GT (Q2PGW5), *Scutellaria baicalensis* 7GT (Q9SXF2), *Solanum melongena* 5GT (Q43641), *Torenia hybrida* 5GT (Q9ZR25), *Verbena hybrida* 5GT (Q9ZR25), *Vitis vinifera* 3GT (P51094), and *Zea mays* 3GT (P16165).

Supplementary Figure S7. Phylogenetic tree inferred from the amino acid sequences of MalT from *Cymbidium* hybrid and other species.

The phylogenetic tree of BAHD acyltransferase proteins was constructed by the neighbor-joining method with 1,000 bootstrapping data sets. MalT name and GenBank accession number are indicated as described previously [51].

Figure 1


A
S
P
P
C
L
S
S
B
S1
S2
S3
S4

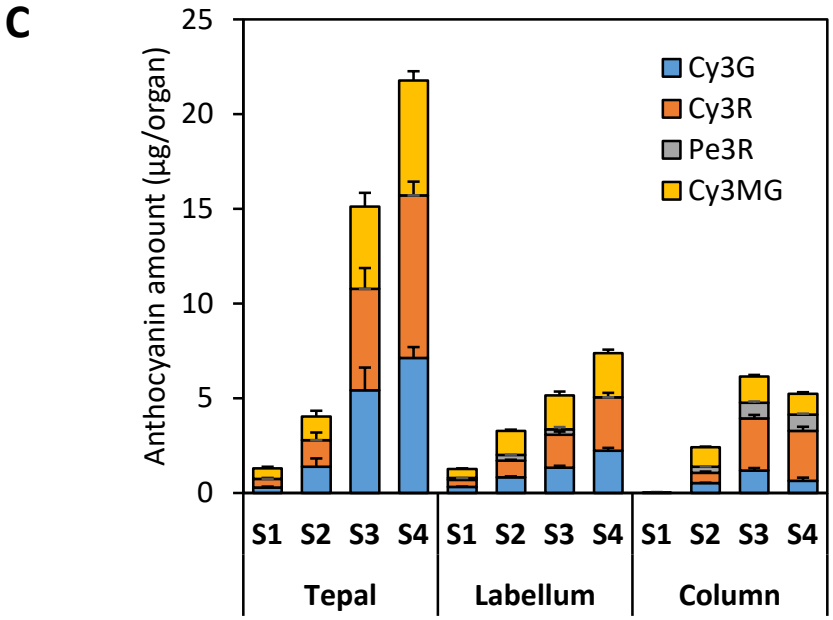
C
Anthocyanin amount (µg/organ)
25
20
15
10
5
0
Cy3G
Cy3R
Pe3R
Cy3MG
S1 S2 S3 S4 S1 S2 S3 S4 S1 S2 S3 S4
Tepal
Labellum
Column

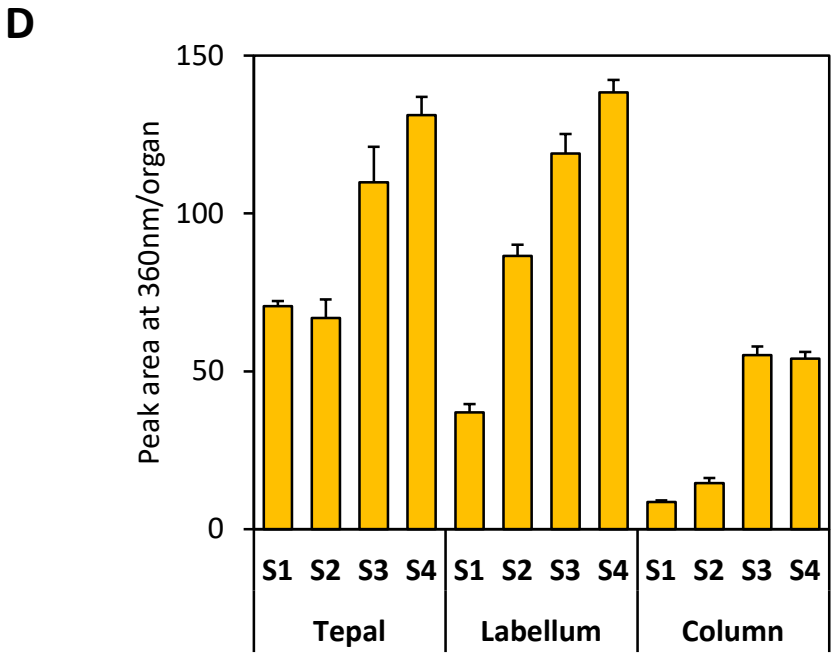
D
Peak area at 360nm/organ
150
100
50
0
S1 S2 S3 S4 S1 S2 S3 S4 S1 S2 S3 S4
Tepal
Labellum
Column

Figure 2

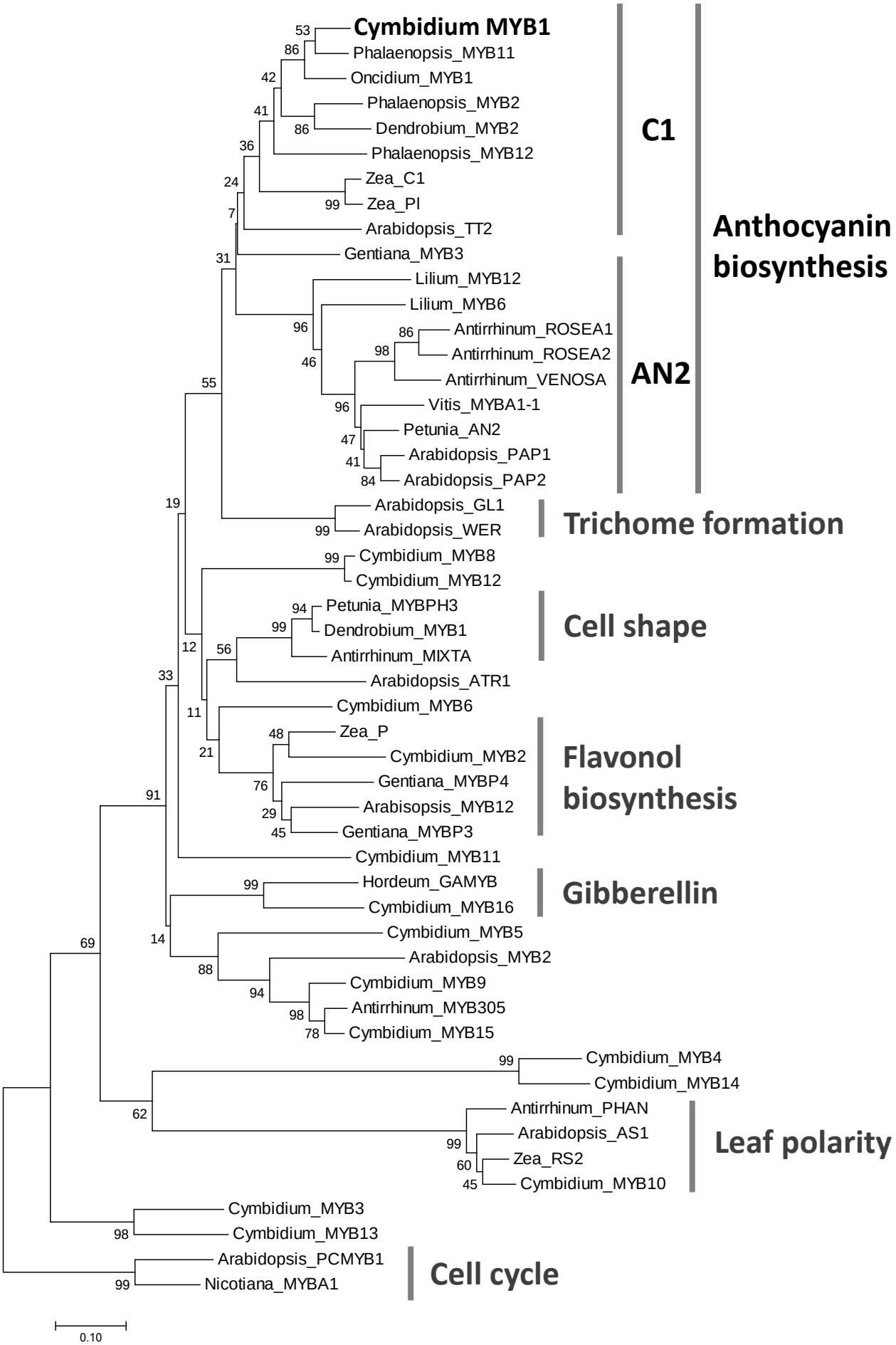
Cymbidium MYB1
Phalaenopsis_MYB11
Oncidium_MYB1
Phalaenopsis_MYB2
Dendrobium_MYB2
Phalaenopsis_MYB12
Zea_C1
Zea_PI
Arabidopsis_TT2
Gentiana_MYB3
Lilium_MYB12
Lilium_MYB6
Antirrhinum_ROSEA1
Antirrhinum_ROSEA2
Antirrhinum_VENOSA
Vitis_MYBA1-1
Petunia_AN2
Arabidopsis_PAP1
Arabidopsis_PAP2
Arabidopsis_GL1
Arabidopsis_WER
Cymbidium_MYB8
Cymbidium_MYB12
Petunia_MYBPH3
Dendrobium_MYB1
Antirrhinum_MIXTA
Arabidopsis_ATR1
Cymbidium_MYB6
Zea_P
Cymbidium_MYB2
Gentiana_MYBP4
Arabisopsis_MYB12
Gentiana_MYBP3
Cymbidium_MYB11
Hordeum_GAMYB
Cymbidium_MYB16
Cymbidium_MYB5
Arabidopsis_MYB2
Cymbidium_MYB9
Antirrhinum_MYB305
Cymbidium_MYB15
Cymbidium_MYB4
Cymbidium_MYB14
Antirrhinum_PHAN
Arabidopsis_AS1
Zea_RS2
Cymbidium_MYB10
Cymbidium_MYB3
Cymbidium_MYB13
Arabidopsis_PCMYB1
Nicotiana_MYBA1
C1
AN2
Anthocyanin biosynthesis
Trichome formation
Cell shape
Flavonol biosynthesis
Gibberellin
Leaf polarity
Cell cycle
0.10

Figure 3

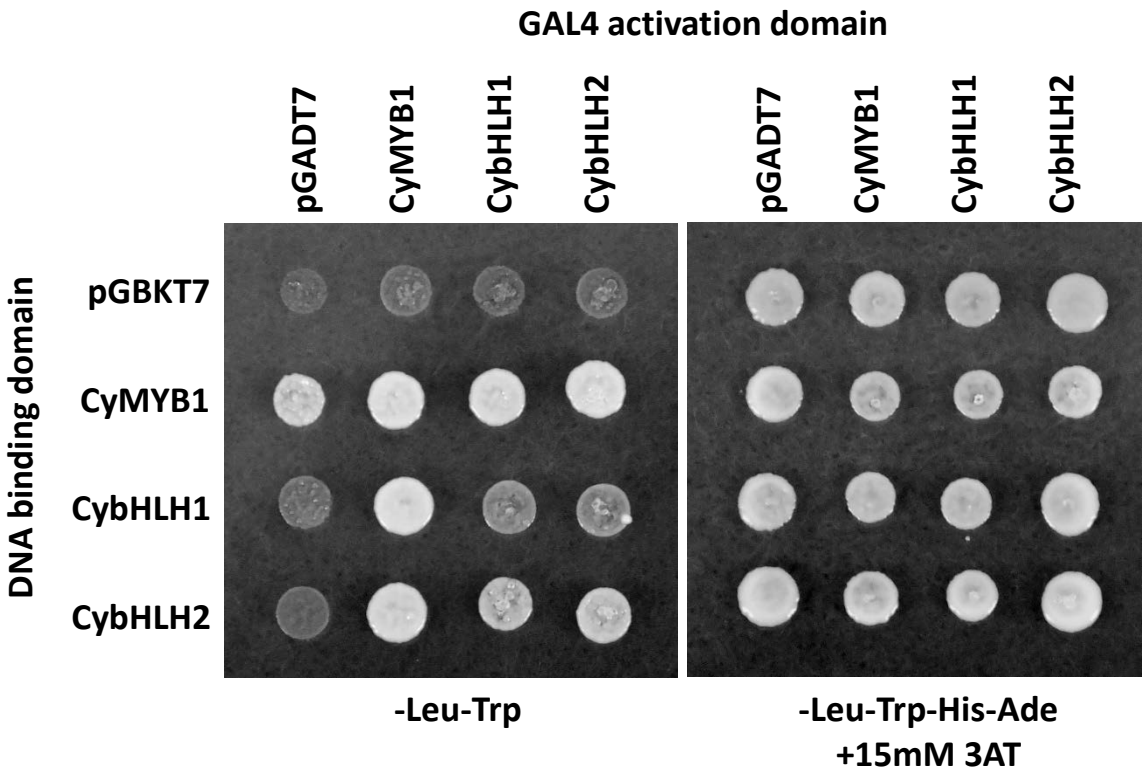
GAL4 activation domain
pGADT7
CyMYB1
CybHLH1
CybHLH2
pGADT7
CyMYB1
CybHLH1
CybHLH2
DNA binding domain
pGBKT7
CyMYB1
CybHLH1
CybHLH2
-Leu-Trp
-Leu-Trp-His-Ade
+15mM 3AT

Figure 4

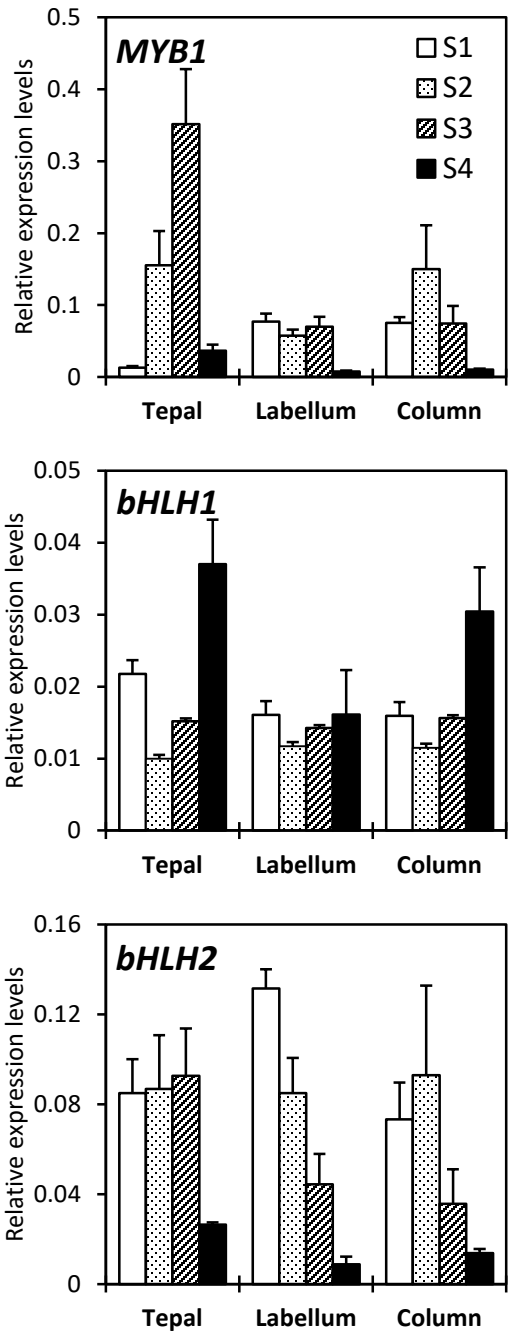
MYB1
S1
S2
S3
S4
Relative expression levels
0.5
0.4
0.3
0.2
0.1
0
Tepal
Labellum
Column
bHLH1
Relative expression levels
0.05
0.04
0.03
0.02
0.01
0
Tepal
Labellum
Column
bHLH2
Relative expression levels
0.16
0.12
0.08
0.04
0
Tepal
Labellum
Column

Figure 5

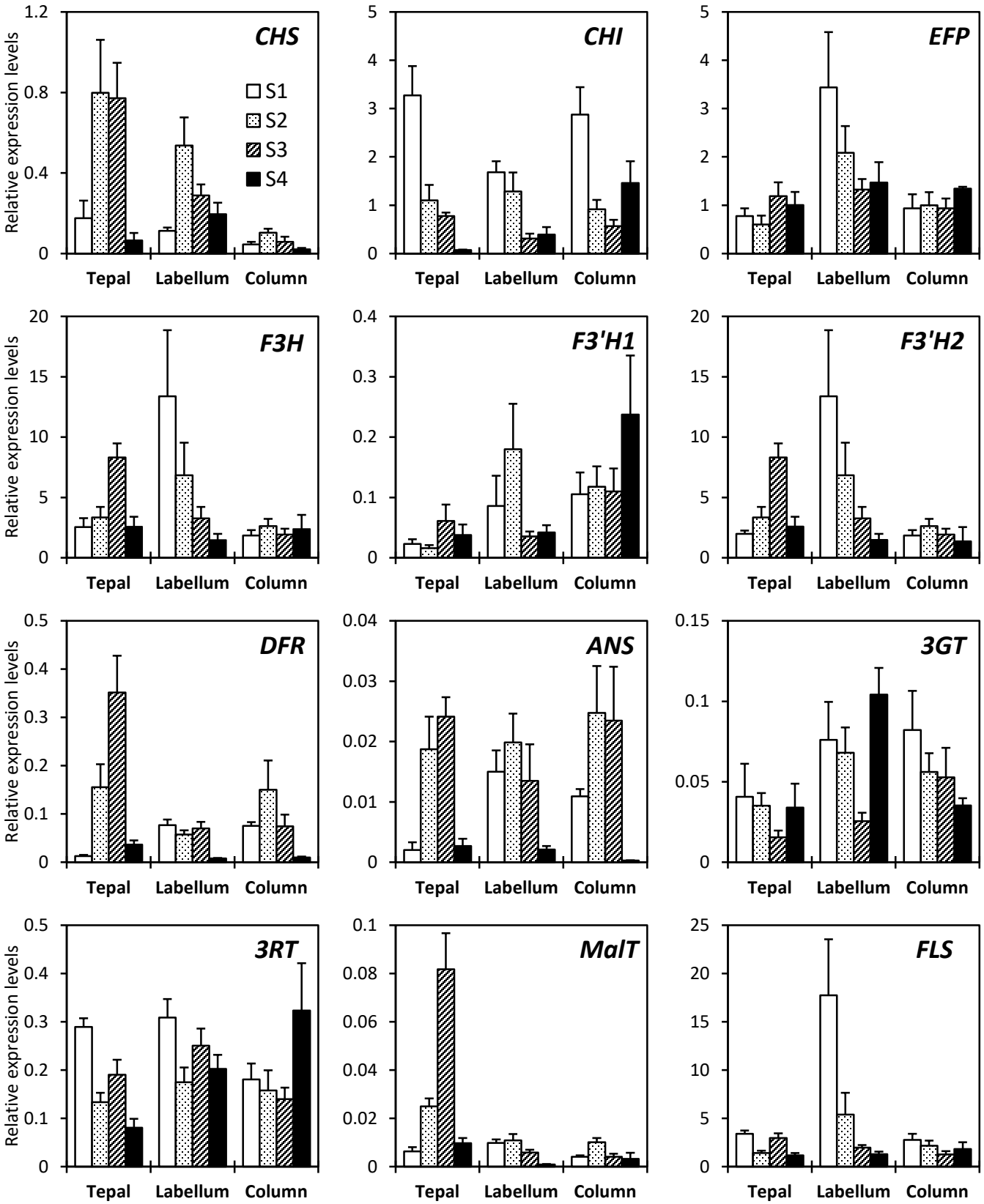
CHS
CHI
EFP
F3H
F3'H1
F3'H2
DFR
ANS
3GT
3RT
MalT
FLS
S1
S2
S3
S4
Relative expression levels
Tepal
Labellum
Column

Figure 6

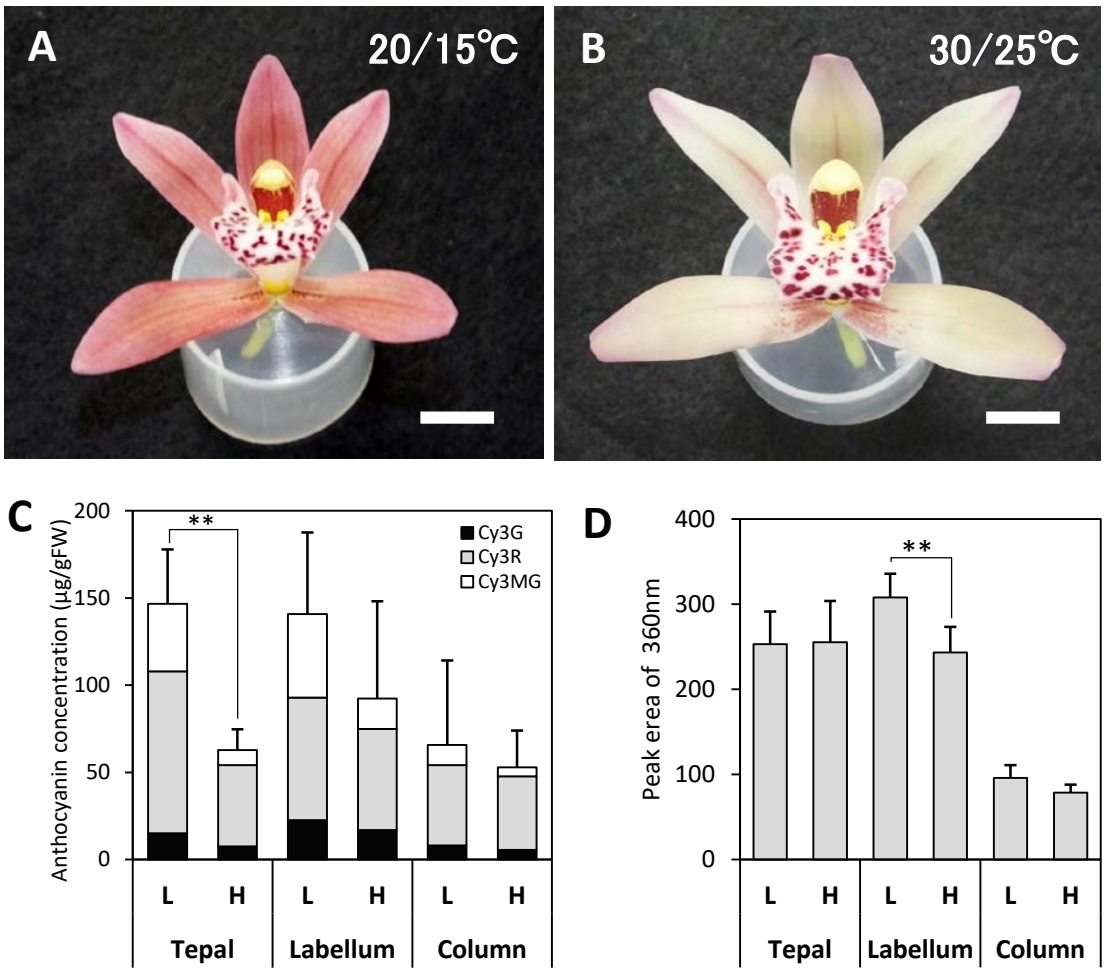
A
20/15℃
B
30/25℃
C
Anthocyanin concentration (μg/gFW)
200
150
100
50
0
**
Cy3G
Cy3R
Cy3MG
L
H
L
H
L
H
Tepal
Labellum
Column
D
Peak erea of 360nm
400
300
200
100
0
**
L
H
L
H
L
H
Tepal
Labellum
Column

Figure 7

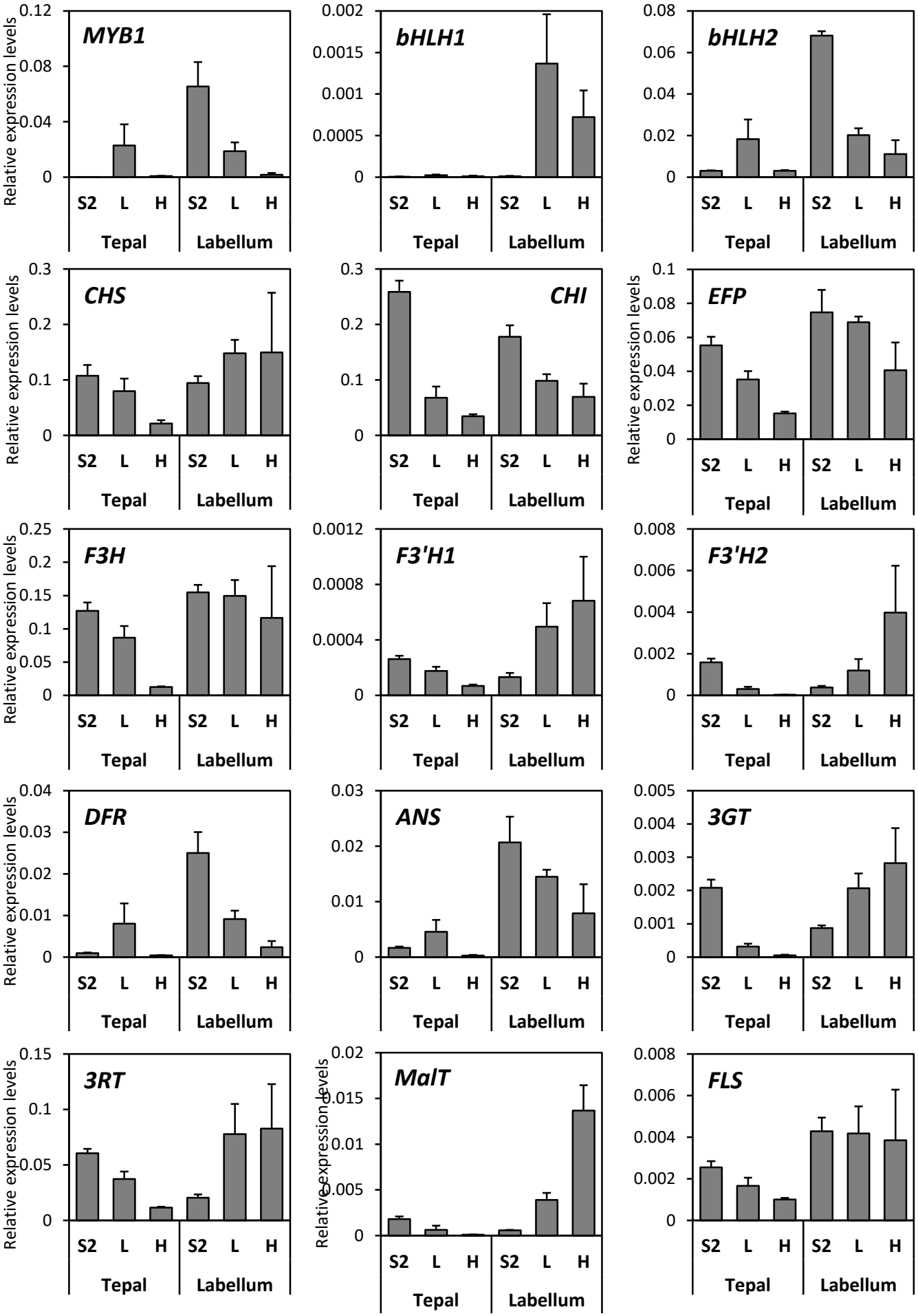
MYB1
bHLH1
bHLH2
CHS
CHI
EFP
F3H
F3'H1
F3'H2
DFR
ANS
3GT
3RT
MalT
FLS
Relative expression levels
S2 L H S2 L H
Tepal
Labellum

Supplementary Figure S1

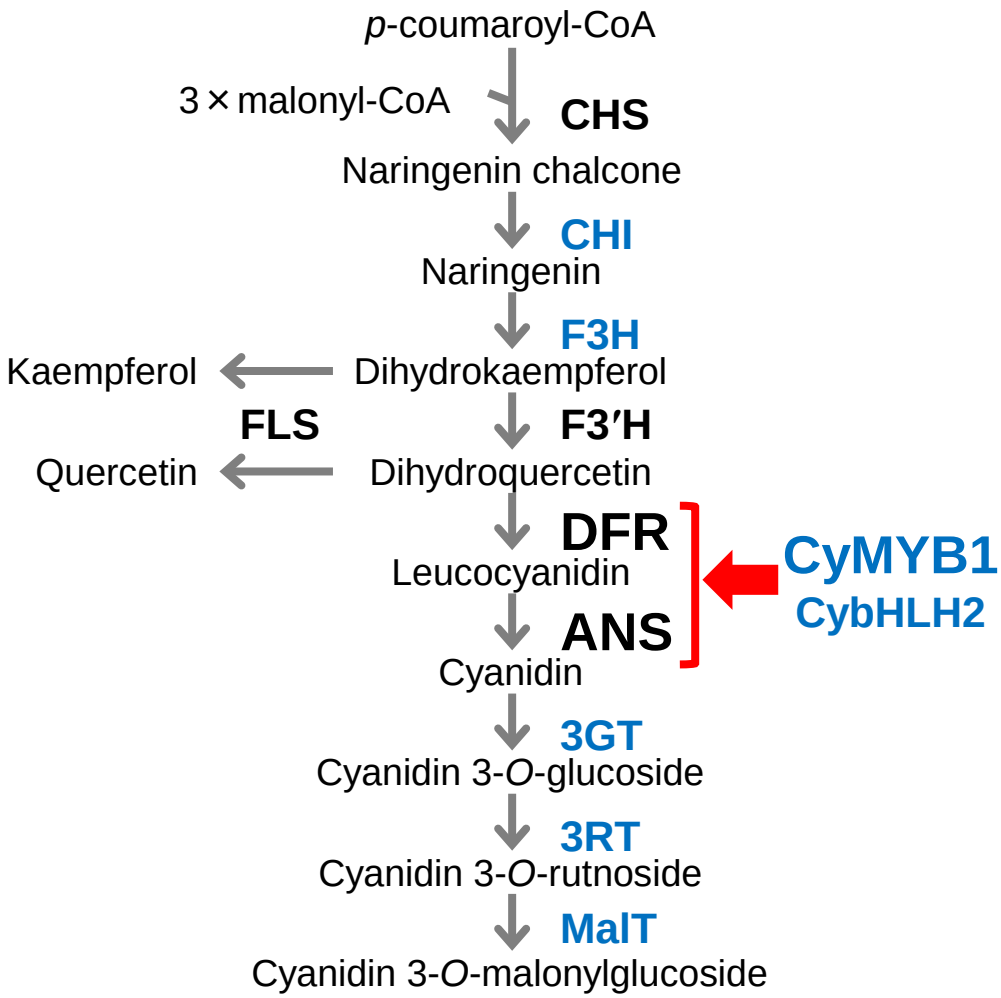

Supplemental Figure S2

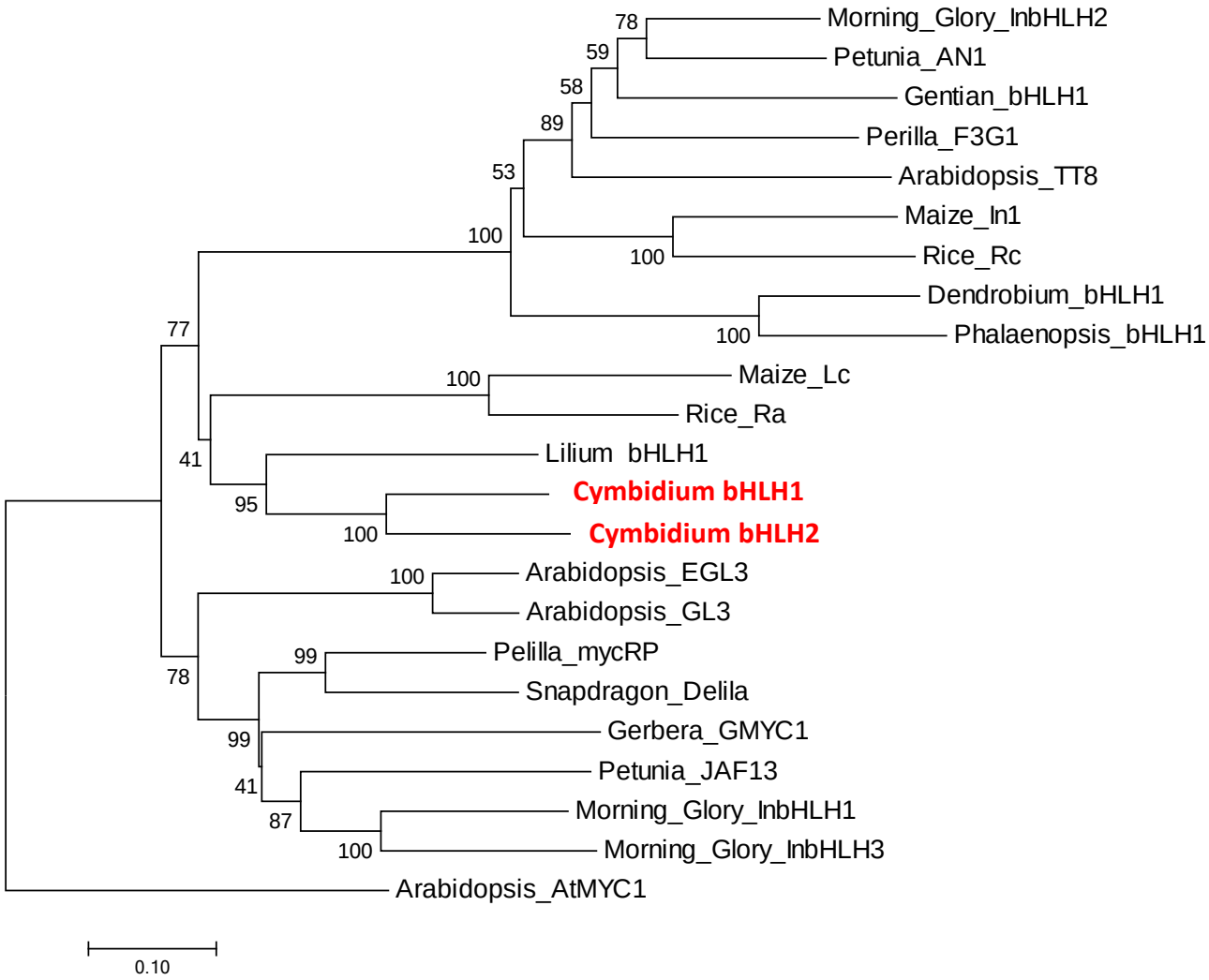

Supplemental Figure S3

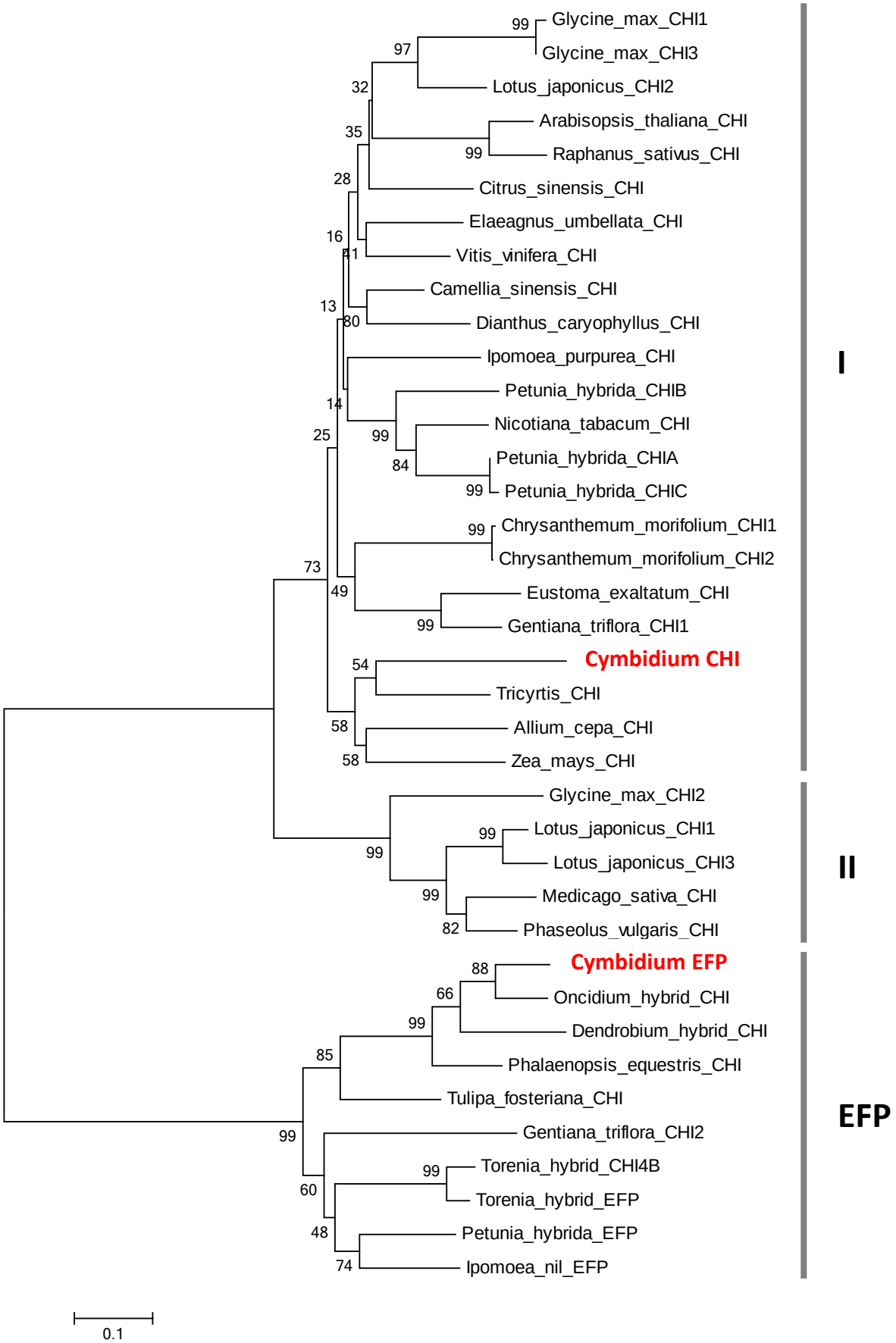

Supplemental Figure S4

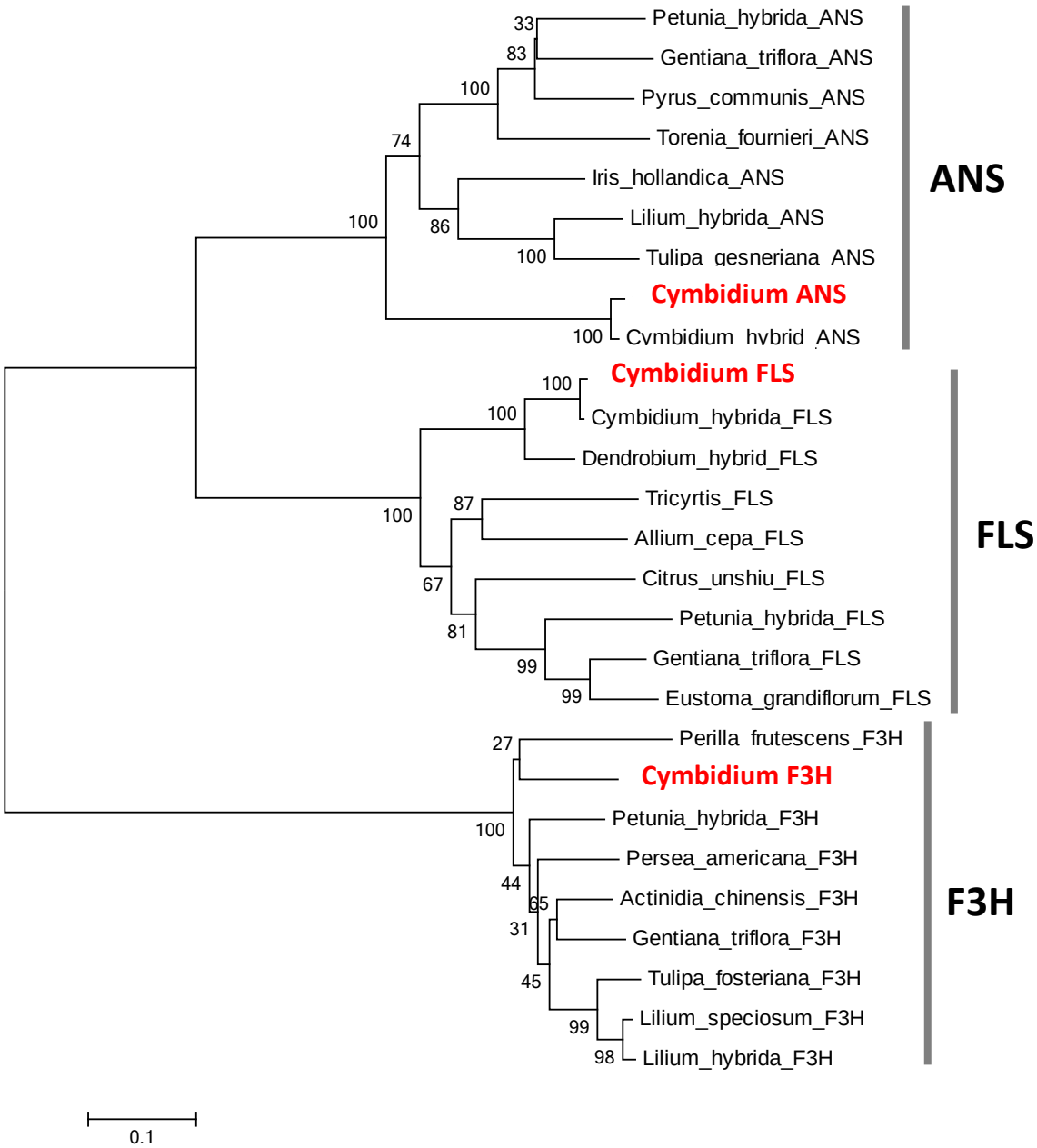

Supplemental Figure S5

A

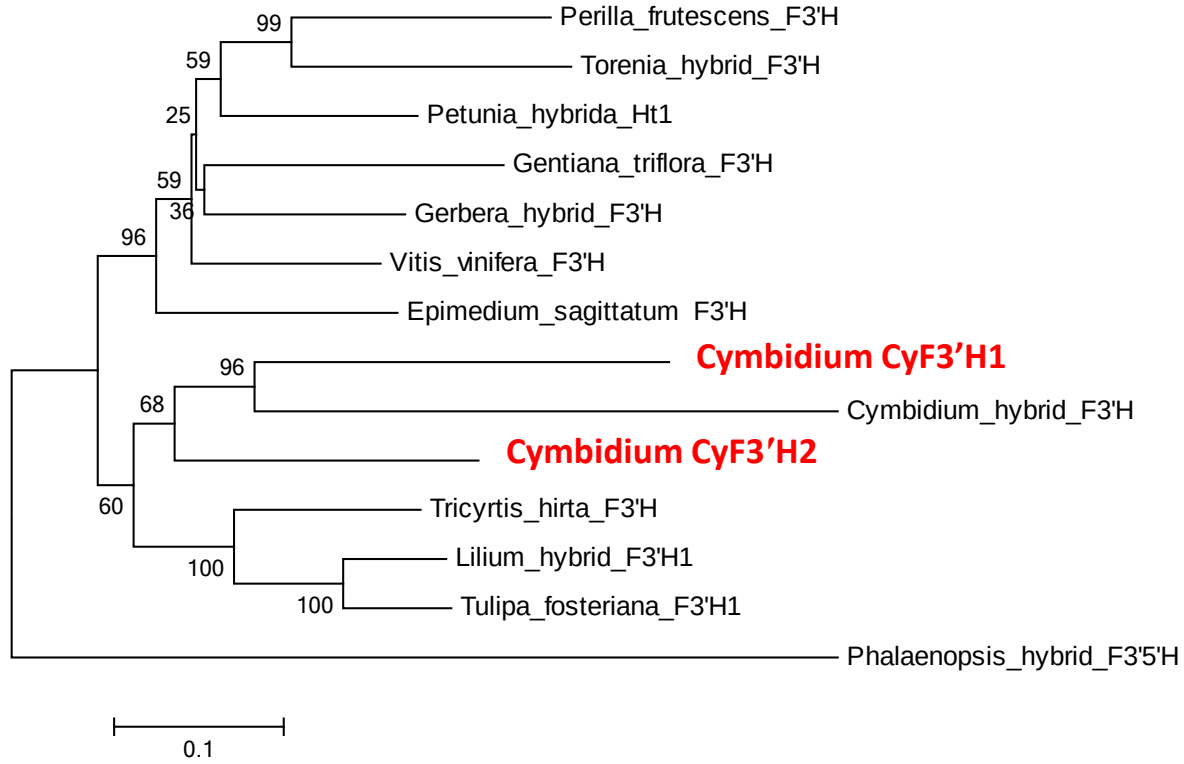

B

```
CyF3'H1  MAILS--LLL VPLLLLLSAI LLARRIRPHR QSKLPLPPGP KGSPILGNLL QLGPKPHETL YNLSKSYG-- PLIHLRFGFV
CyF3'H2  MALVI--FVL FATILFASLL FIVISG-DRR RGRSNLPPGP KGWPIIGNLP QLGPKPHQTL YALAKTYG-- PILRLRLGAV
ChF3'H   MAVIFTFLVF FISVLLLSSL FLVGTG---R RRRPPLPPGP KGWALLGNLL QLGTKPHRTL QALSQSHGSA GLLRLRLGTV
         **::   ::: .  :*: * : ::.      * : :  ***** ** .::***  ***.***.**   *::::*    :::**:* *

CyF3'H1  DMIVVNSAAI AAKILR-NDA NVASRPSSTS VKHIAYNHQD LIFARYGARW RMLRKICALQ LFSPKAMEDL APVRADEVGR
CyF3'H2  DVVVASSAAA ASQFLRTHDA NFSSRPPNSG AEHVAYNYQD LVFAPYGARW RMLRRLCVSH LFSAKAMEDF RHVRGGEVER
ChF3'H   DAIVISSASA AAKCFRSHDA ILTSRPPNSV GKYITYNFED LIMAPYGPRW QMLRKVCSTH LLSTKALDSF RHVWDEDVAM
         * :* .**:  *:: :* :**  .:***..:   :::***.:* *::* **.** :***::*  : *:*.**::.:   *   :*

CyF3'H1  FVRELVKEE- KFVDLSDGIS ACAADALSRV VVGKRVFGDG EE---SREFK EMVMEMMNLS SAFNINDFVP GLGWLDVQGL
CyF3'H2  LVHGIAEEEG VAVDVGGAVN TCTTNALTQV TVGRRVFGGR EEKEGAEEFK EMVVELMNLA GVFNFGDFVP GLGWLDLQGV
ChF3'H   DVRELTSGRE AAVDVGGLVN TCVTNALAHV LIGRQEIVGG EE---AAEFK EIAAEMTTLA GQFNVGHFIP WIGWLDLQDL
          *: :.. .    **:.. :. :*.::**::*  :*:: : .  **   : *** *:. *: .*: . **...*:*  :****:*.:

CyF3'H1  VAKMKKLHRK FDEFLDKVIE DHKARLTETE NATTAAAAGG RGRHNDLLSV LIEAKGDANG DGIALTDADI KPLLQNMFAA
CyF3'H2  VRKMKKLHKR FDKLFDGIIA EHRESVEKGD -------VHG RG--SDMLSI LLRLKEEADG EGNLLTDTNI KALLLNLFAA
ChF3'H   NKKMMKSRVR FGEFLEKIIE EHSS------ --------KG IDYAKDFLSV LIQINGEPNA KHDELTNINI KALLQDMFIA
           ** * : : *.:::: :*  :*                 *  .  .*:**: *:. : :.:. .   **: :* *.** ::* *

CyF3'H1  GTDTSSNTIE FAIAELIRHP ELLVRAQQEL DSVVGRRRLV AESDLPNLPF FQAVVKETFR HHPAAPLSLP RIISEDYEID
CyF3'H2  GTDTTSSTVE WAMAELIRHP NLLKQAQTEL DSVVGHNRLV SESDLPNLPF LQAIVKETFR LHPSTPLSLP RVASSDCEID
ChF3'H   GTDTTSITIE WLLSELLRHP HILARAQHEL DSVAGRNRLI SQSDLPKVPF LDAIVKETLR LHPPVPLSVP RMATEDCEID
         ****:* *:* : ::**:*** .:* :** ** ***.*:.**: ::****::** ::*:****:*  **..***:* *: :.* ***

CyF3'H1  GYLIPKGATL LINIWAIGRD PIAWADETLA FQPDRFLPGG RHEGADVKG- NDFELIPFGG GRRICAGMNL GLRMVQLLSA
CyF3'H2  GHLIPRGATL LVNVWSIGRD PSMWPDEPLA FRPGRFLAGG RHEGVDVKG- NDFELIPFGA GRRICVGLSL GLRMVQFMTA
ChF3'H   GYLIPKGAYL LVNIWAIGRD LATWHDDPNE FDPDRFVPGS PHESADVKGI NNFELIPFGA GRRRCAGTKL GIRMVHFVTA
         *:***:** * *:*:*:****    * *:.   * *.**:.*.  **..****  *:*******. *** *.* .* *:***::::*

CyF3'H1  TLVHAFDWKL PEGELPEKLD MDLSFGLTLH RTNPLMIRPV PRLEPEAYV- --
CyF3'H2  TLIHAFDWEL AGGETAEKLD MEEAYGLTLR RAAPLVAKPT TRLALKAYPK HV
ChF3'H   MMLHAFDWTL PDGSMGDLLD MEESYGATMP KTRPLMAKAT PRLAPQAYL- --
          ::***** * . *.  : ** *: ::* *:  :: **: :.. .**  :**
```

Supplemental Figure S6

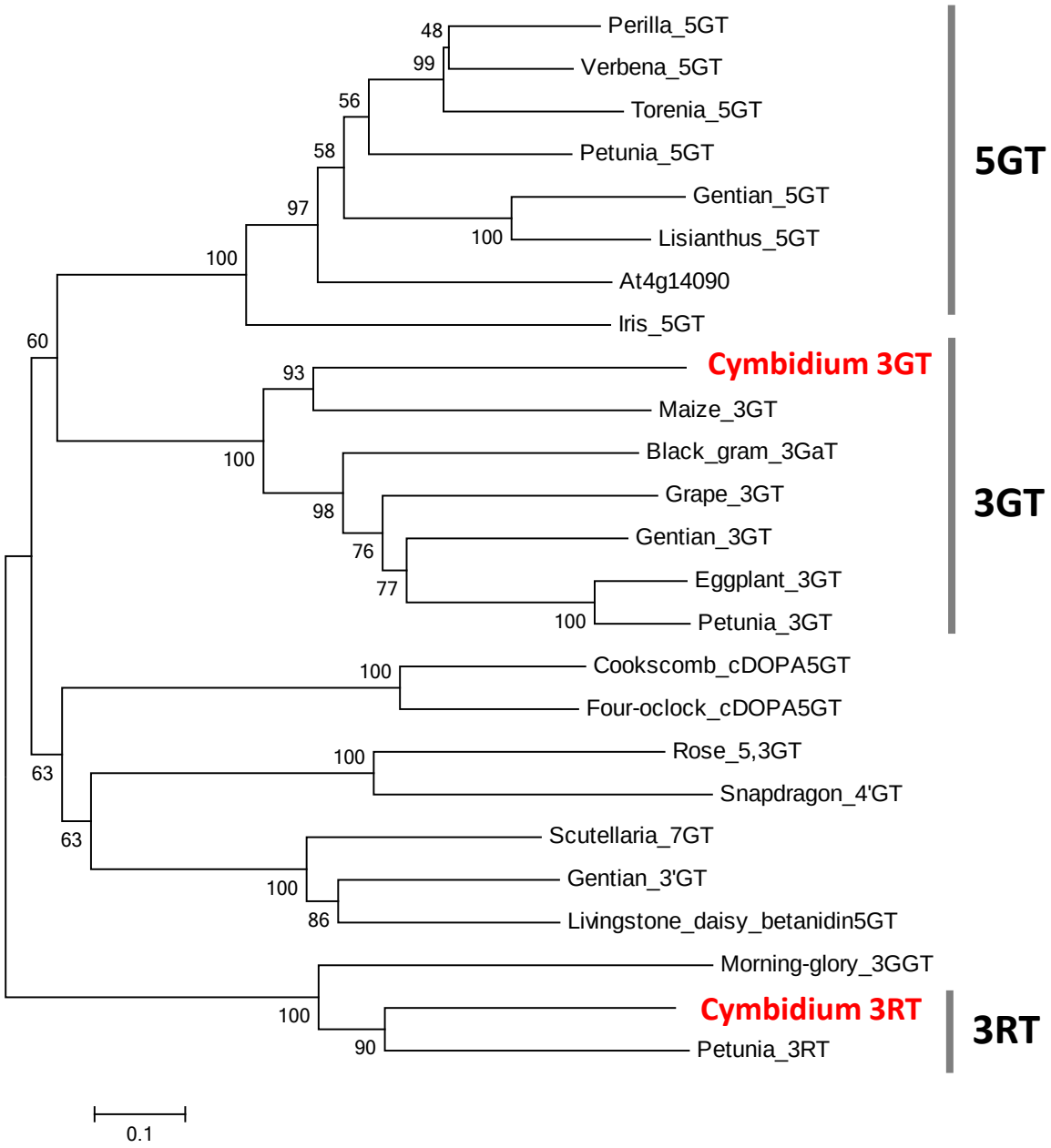

Supplemental Figure S7

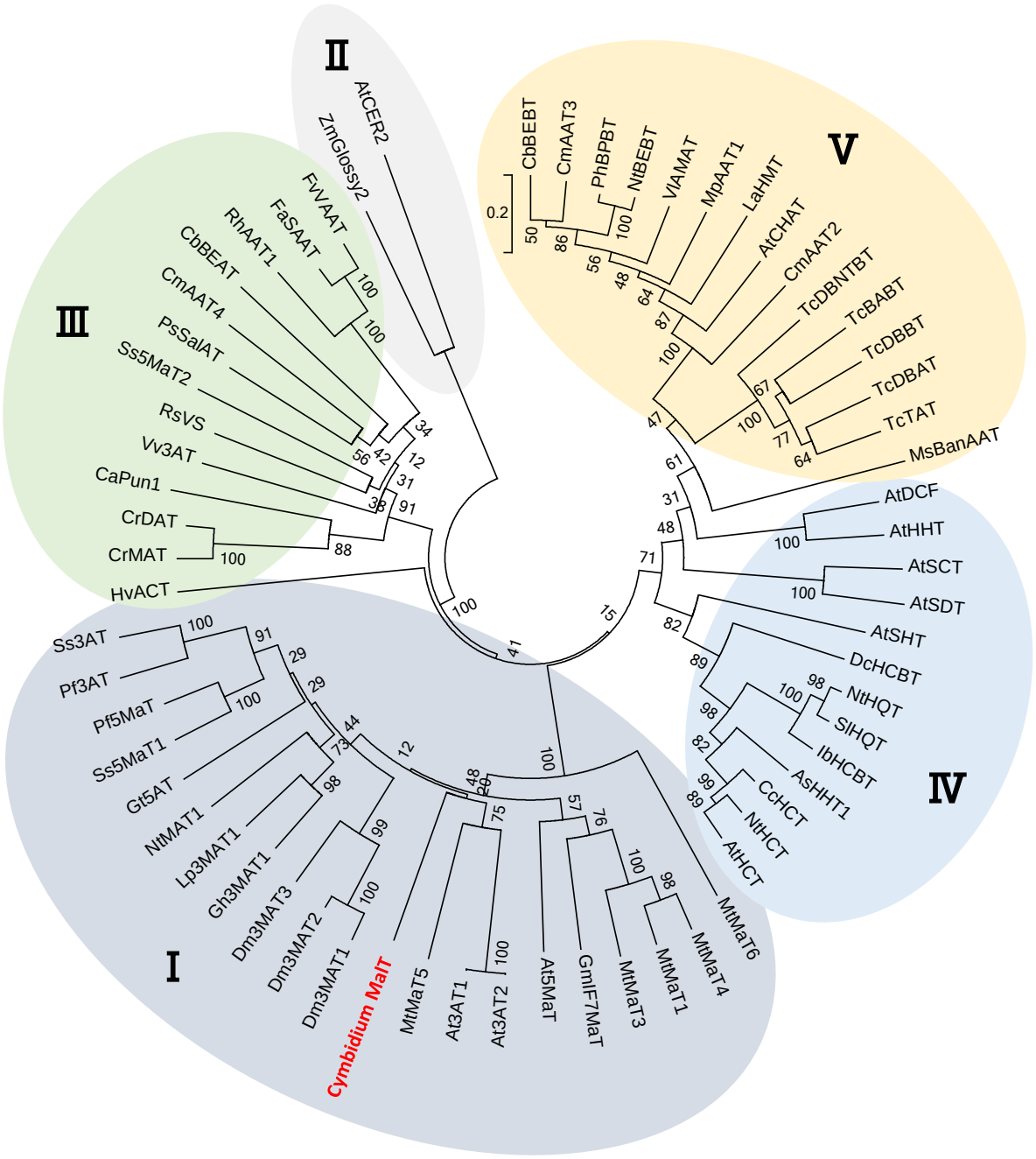

Supplemental Table S1 Primer sequence used in ORF amplification

	Sequences (5′→3′)	
	Forward	Reverse
CyMYB1	ATGAAGAAGAAGCCATTCTGTGACG	TTAAAAATTCATCCAAATATCTGTCTCC
CybHLH1	ATGGCGGTAGATATGCAGAGCCAAGAAG	TTAACATTTGCTGACGGCTCTCTG
CybHLH2	ATGCAGACCCAAGAGGAGCTGCAG	TTAACATTTGCTGACGGCTCTCTG
CyCHI	CGACATGGCAGAAACGCCGGCAAC	TCAAGCGACCTCAACTTGCTCGAAC
CyEFP	ATGAGTTCGAAAGAGGTGATGATAG	CTATTTTGACAATATTGCTTCAAATTTCTC
CyF3H	ATGGCGCCAGTACAATTCCTCCCCAC	TTAAGCTAGAATTTCGTTTAATGTC
CyF3′H1	ATGGCCATTCTCTCCCTCCTCCTCGTAC	TCAAACATAAGCCTCCGGTTCAAGCCGG
CyF3′H2	ATGGCTCTCGTAATCTTCGTCCTCTTCG	TTAGACATGCTTAGGATATGCCTTTAGG
CyANS	ATGGCCACCAGAACCATCCCCGCTAC	TCACGACCCGTCGCCTGCTTCCTC
Cy3GT	ATGGTCCTCTCTAGCGATTCATCTCCGC	TCAATTTCTGCAAACCAACGCCACCAG
Cy3RT	ATGGCCAACAACGATGAAGTTACGGCC	TCACTTGGATGATTTATCATAAGCCAA
CyMalT	ATGGCATCTTTAAGAATACTCG	TCAAGCCCACCTAGTAAGAAAC
CyFLS	ATGGAGGTGGAAATACAGAGAGTCCAATC	TCACTGCGGCAGCTTGTTGATTTTGCAG

Supplemental Table S2 Primer sequence used in qRT-PCR analysis

	Sequences (5′→3′)	
	Forward	Reverse
CyMYB1	GAGCCAAAATTAAAACCTCAAGAA	CATTGATTCATCTCCAAAGTTCTG
CybHLH1	TACCCAGATATTGCAGAAAGAACA	TGGCTTCAATTATGTCAAGGAGTA
CybHLH2	CATCAATAGACTGAATGAGCCATC	CTTCCTCAATTCCTAAAGAACCAA
CyCHS	CCGGACTACTACTTCAGAATCACA	TCAGAATCTCTTCCGTTAGGTACA
CyCHI	CCGAGACATAATTACAGGTTCCTT	GAATGAGTGAAGATGATGGAAGTG
CyEFP	GAAGAAGGATTCTGTGATCACCTT	GCATTCTCCACTTGGATCTTACTT
CyF3H	CGTGAAGCTCTAACCCAAGC	CTGAACGGTGATCCAGGTTT
CyF3'H1	ATTTGATGAATTTTTGGACAAGGT	TTCGCTTCTATCAGCACACTTAAC
CyF3'H2	TGAAGAAGCTGCATAAAAGATTTG	TCAGTAAGAGAGCCTTGATGTTTG
CyDFR	GAAAGCTTCGACGAGGTGAC	GGTGTTCCTCCACGTTCACT
CyANS	GATTCAGGGCTATGGAAGCA	TCCTCAGCAAAAGAGGTCGT
Cy3GT	TTCGGCGATTCTAACTCTAAATTC	AACTGAAGAGAGTTCATGGGAGTC
Cy3RT	AAGCTAGTGCTGTTACCGCTTAGA	CATCCAAGAAAAACTCTCTCCACT
CyMalT	CCTACTCTCCGCCATGGAAATAGA	CGATTGTGGAGATTGGAGATGATG
CyFLS	AGGATAAGTATGCGATGAAGGAAG	CCCTCTAGAAAGCCACTTCAATAG
CyACT1	TTGTTAGGGACATAAAGGAGAAGC	ATTTCATGATGGAGTTGTATGTGG